

Metrics and stabilization in one parameter persistence^{*}

Wojciech Chachólski[†] Henri Riihimäki[‡]

March 2, 2022

Abstract

We propose the use of persistent homology in a supervised way. We believe homological persistence is fundamentally not about decomposition theorems but a central role is played by a choice of metrics. Choosing a pseudometric between persistent vector spaces leads to a model. Fitting this model is what we believe supervised homological persistence is. We develop theory behind constructing such models and we give evidence of the usefulness of this approach in concrete data analysis tasks.

1 Sense of geometry

During the last decade there has been a considerable increase in research focused on persistent homology. This has been fueled by an explosion of applications ranging from neuroscience [12], to vehicle tracking [2], and the characterization of nanomaterials [13], testifying to usefulness of homology to understand spaces described by measurements and samplings. All these applications of persistent homology have been in principle exploratory in nature with some elements of learning based on persistent diagrams. In fact, persistent homology can be regarded as a generalization to higher homologies of clustering methods (H_0 persistence) that have been the core of exploratory data analysis for a long time. Although exploratory tools are important, the main research front in modern data science has shifted from exploratory to supervised learning, due to even more spectacular applications of machine learning methods.

Our aim in this paper is to explain how to use persistent homology in a supervised way, allowing to optimize over various models for the observed homological information. The focus is on studying the space of stable translations from homological information into information that can be analysed through more basic operations such as counting and integration enabling the use of statistical tools to its outcomes. We show how a pseudometric on the set $\text{Tame}([0, \infty), \text{Vec}_K)$ of tame $[0, \infty)$ -parametrized K vector spaces (see Section 3), which is a natural place where homological invariants of data live,

^{*}First author was funded by VR and Göran Gustafsson foundation. Second author was partly supported by a collaboration agreement between the University of Aberdeen and EPFL.

[†]Mathematics Department, KTH, S-10044 Stockholm, Sweden. (wojtek@kth.se).

[‡]Mathematics Department, University of Aberdeen, Aberdeen AB243UE, Scotland, UK. (henri.riihimaki@abdn.ac.uk).

leads to a stable translation. Every such pseudometric gives therefore a model for extracting information from persistent homology. Fitting this model to the training data is what in our approach persistence based supervised learning is. In Section 10 of the paper we illustrate that this strategy can indeed lead to improvements in classification tasks. We consider two such tasks: distinguishing between random point processes on a unit square generated according to different distributions, and distinguishing between activities of ascending and descending stairs of 7 people based on the activity monitoring PAMAP2 data obtained from [14]. By choosing a different model, in the first case the overall averaged accuracy improves from 73% to 78% and in the second case from 60% to 65%. Our goal for this paper however is not to benchmark our approach. Our goal is to present the proof of concept of the key ideas, explain their mathematical background, and indicate that they can lead to improvements in analysing data. Discussing the effectiveness of this approach is planned for a sequel to this article.

Our models are built using a process called **hierarchical stabilization of the rank** which assures the necessary stability requirement. It builds on work presented in [6], [7], and [17]. The input to the process is a pseudometric d on the set $\text{Tame}([0, \infty), \text{Vec}_K)$. The output is a Lipschitz-continuous function $\widehat{\text{rank}}_d: \text{Tame}([0, \infty), \text{Vec}_K) \rightarrow \mathcal{M}$ where \mathcal{M} is the space of Lebesgue measurable functions $[0, \infty) \rightarrow [0, \infty)$ in which probability and statistical methods are well developed. We think about this function as the model associated to the pseudometric d . In this framework (supervised) persistence analysis is about identifying these pseudometrics d for which structural properties of the (training) data are reflected by the geometry of its image in \mathcal{M} through the function $\widehat{\text{rank}}_d$. The strategy of looking for appropriate pseudometrics can only work if we are able to parametrize explicitly a rich subspace of pseudometrics on $\text{Tame}([0, \infty), \text{Vec}_K)$. Such rich parametrizations would enable the use of for example stochastic gradient descent techniques to search through the parameters for suitable pseudometrics, which we intend to explore in the mentioned sequel to this paper. This article builds on our discovery that such parametrizations are indeed possible using Lebesgue measurable functions $[0, \infty) \rightarrow (0, \infty)$ with positive values referred to as densities (see 5.4 and 5.5).

Parametrizing models for persistence analysis by pseudometrics should not be surprising. Discovering appropriate metrics and units to measure physical phenomena is essential in understanding these phenomena. Comparison and interpretation of observations should depend on the phenomena and the experiments they came from and not simply just on their values. Different phenomena might require different comparison metrics. We should not restrict ourselves to only bottleneck or Wasserstein distances to compare outcomes of persistence analysis of diverse data sets obtained from a variety of different experiments. We should be able to choose metrics that fit particular experiments. Our goal is to present mathematical foundations of how to do it for outcomes of persistent homology. This fits also well with many recent studies ([3], [8], [19], [18], [20]) which challenge the traditional view in persistence that bars with long lifespans are of importance and smaller bars are to be considered as noise. These studies show that also shorter bars and their appearance in the filtration might carry important information. For example in [8] the authors find that observed diffraction peaks of amorphous silica glass relate to small scale

loops in the atomic configurations. It thus depends on the analysis at hand what is to be taken as noise and we advocate that emphasizing the meaningful features is a question of choosing an appropriate metric on $\text{Tame}([0, \infty), \text{Vec}_K)$.

2 Hierarchical stabilization

All the proofs of the propositions presented in this section are placed in Appendix A.

A discrete invariant is a function $R: T \rightarrow \mathbf{N}$ with values in the set of natural numbers $\mathbf{N} = \{0, 1, \dots\}$. We think about T as a collection of data sets or objects that represent them. If T consists of finite metric spaces for example, such an invariant might assign to a metric space in T the number of clusters obtained by applying some clustering algorithm. Our method of converting such a discrete invariant into a stable one, which we call **hierarchical stabilization**, requires a choice of a pseudometric d on T and this is the key step central to persistence analysis in our approach. Recall that a pseudometric is a function $d: T \times T \rightarrow [0, \infty]$ satisfying reflexivity $d(X, X) = 0$, symmetry $d(X, Y) = d(Y, X)$ and triangular inequality $d(X, Y) + d(Y, Z) \geq d(X, Z)$ for any X, Y , and Z in T . Here $[0, \infty]$ denotes the extended set of non-negative real numbers including ∞ with the standard arithmetic and order relation. Its subset of real numbers is denoted by $[0, \infty)$.

Once a pseudometric d on T is chosen, for X in T , we define $\widehat{R}_d(X): [0, \infty) \rightarrow [0, \infty)$ to be the function given by the formula:

$$\widehat{R}_d(X)(t) := \min\{R(Y) \mid d(X, Y) \leq t\}.$$

The number $\widehat{R}_d(X)(t)$ is the minimum among all the values R takes on the disk $B_d(X, t) := \{Y \mid d(X, Y) \leq t\}$ around X with radius t with respect to the pseudometric d . This function is non-increasing with values in natural numbers and hence Lebesgue measurable. Furthermore there is t such that, for $s \geq t$ in $[0, \infty)$, the equality $\widehat{R}_d(X)(t) = \widehat{R}_d(X)(s)$ holds. This value $\widehat{R}_d(X)(t)$ is called the **limit** of $\widehat{R}_d(X)$ and is denoted by $\lim(\widehat{R}_d(X))$. Recall that \mathcal{M} denotes the set of Lebesgue measurable functions $[0, \infty) \rightarrow [0, \infty)$.

Definition 2.1. Hierarchical stabilization of $R: T \rightarrow \mathbf{N}$ with respect to a pseudometric d on T is the function $\widehat{R}_d: T \rightarrow \mathcal{M}$ that maps X in T to $\widehat{R}_d(X)$.

The range \mathcal{M} of \widehat{R}_d has a much richer geometry than the set of natural numbers, the range of R . For example, \mathcal{M} has many interesting pseudometrics, among them the standard L_p -metric (for $p \geq 1$) and a so called **interleaving** metric d_{\bowtie} :

$$\begin{aligned} L_p(f, g) &:= \left(\int_0^\infty |f(t) - g(t)|^p dt \right)^{\frac{1}{p}} \\ S &:= \{\epsilon \mid f(t) \geq g(t + \epsilon) \text{ and } g(t) \geq f(t + \epsilon) \text{ for all } t \in [0, \infty)\} \\ d_{\bowtie}(f, g) &:= \begin{cases} \inf(S), & \text{if } S \text{ is non-empty} \\ \infty, & \text{otherwise.} \end{cases} \end{aligned}$$

The hierarchical stabilization satisfies the following Lipschitz properties:

Proposition 2.1. Let d be a pseudometric on T , $R: T \rightarrow \mathbf{N}$ a function, and $p \geq 1$ a real number. Then, for X and Y in T :

1. $d(X, Y) \geq d_{\bowtie}(\widehat{R}_d(X), \widehat{R}_d(Y))$.
2. $c d(X, Y)^{\frac{1}{p}} \geq L_p(\widehat{R}_d(X), \widehat{R}_d(Y))$, where $c = \max\{\widehat{R}_d(X)(0), \widehat{R}_d(Y)(0)\}$.

We think about the hierarchical stabilization as a process of converting a discrete invariant $R: T \rightarrow \mathbf{N}$ into a stable invariant $\widehat{R}_d: T \rightarrow \mathcal{M}$ whose values are in a space in which rich probability and statistical methods are well developed. We take advantage of this in our examples in Sections 10.2 and 10.3. Different pseudometrics on T lead to different invariants. In our framework persistence analysis is about identifying pseudometrics on T for which the associated invariants reflect structural properties of T . The expectation is that some of these properties should be reflected by the geometry of the image of \widehat{R}_d in \mathcal{M} described by the L_p or interleaving metrics if an appropriate pseudometric d on T is chosen. We refer to the function $\widehat{R}_d: T \rightarrow \mathcal{M}$ also as the **hierarchical stabilization model** of T associated to the invariant R and the pseudometric d .

In general there is a loss of information as $\widehat{R}_d: T \rightarrow \mathcal{M}$ may map objects that we do not intend to identify to the same function. For retaining more information we are going to consider families of pseudometrics on T and the induced stabilizations. Let \mathcal{M}_2 denote the set of measurable functions of the form $[0, \infty)^2 \rightarrow [0, \infty)$.

Definition 2.2. Let $R: T \rightarrow \mathbf{N}$ be a function and $\{d_\alpha\}_{\alpha \in [0, \infty]}$ a sequence of pseudometrics on T indexed by $[0, \infty]$.

1. The sequence $\{d_\alpha\}_{\alpha \in [0, \infty]}$ is called **non-decreasing** if $d_\alpha(X, Y) \leq d_\beta(X, Y)$ for all $\alpha < \beta$ in $[0, \infty]$ and X, Y in T .
2. For X in T , $\overline{R}(X): [0, \infty)^2 \rightarrow [0, \infty)$ is a function defined as follows:

$$\overline{R}(X)(\alpha, t) := \widehat{R}_{d_\alpha}(X)(t).$$

3. The sequence $\{d_\alpha\}_{\alpha \in [0, \infty]}$ is called **admissible** for R if $\overline{R}(X): [0, \infty)^2 \rightarrow [0, \infty)$ is Lebesgue measurable for all X in T .
4. Assume $\{d_\alpha\}_{\alpha \in [0, \infty]}$ is admissible for R . Then the function $\overline{R}: T \rightarrow \mathcal{M}_2$, mapping X in T to $\overline{R}(X): [0, \infty)^2 \rightarrow [0, \infty)$, is called the **hierarchical stabilization** of R along the sequence $\{d_\alpha\}_{\alpha \in [0, \infty]}$.

Non-decreasing sequences are key examples of universally admissible sequences:

Proposition 2.2. A non-decreasing sequence $\{d_\alpha\}_{\alpha \in [0, \infty]}$ of pseudometrics on T is admissible for any $R: T \rightarrow \mathbf{N}$.

Similarly to \mathcal{M} , we consider following pseudometrics on \mathcal{M}_2 , the normalized L_p (for $p \geq 1$) and the interleaving metrics:

$$\begin{aligned}\widehat{L}_p(f, g) &:= \lim_{a \rightarrow \infty} \frac{1}{a} \int_0^a \left(\int_0^\infty |f(\alpha, t) - g(\alpha, t)|^p dt \right)^{\frac{1}{p}} d\alpha \\ S &:= \left\{ \epsilon \mid \begin{array}{l} f(\alpha, t) \geq g(\alpha, t + \epsilon) \\ g(\alpha, t) \geq f(\alpha, t + \epsilon) \end{array} \text{ for } (\alpha, t) \in [0, \infty) \times [0, \infty) \right\} \\ d_\infty(f, g) &:= \begin{cases} \inf(S), & \text{if } S \text{ is non-empty} \\ \infty, & \text{otherwise.} \end{cases}\end{aligned}$$

The key parameter in the hierarchical stabilization is the choice of a pseudometric. It turns out that with respect to this key parameter the hierarchical stabilization along a sequence of pseudometrics $\{d_\alpha\}_{\alpha \in [0, \infty]}$ is also stable. Here is one manifestation of this stability:

Proposition 2.3. *Let $R: T \rightarrow \mathbf{N}$ be a function. Assume $\{d_\alpha\}_{\alpha \in [0, \infty]}$ is a non-decreasing sequence of pseudometrics on T . Let $\bar{R}: T \rightarrow \mathcal{M}_2$ be the hierarchical stabilization of R along this sequence. Then, for X and Y in T :*

1. $d_\infty(X, Y) \geq d_\infty(\bar{R}(X), \bar{R}(Y))$.
2. $c d_\infty(X, Y)^{\frac{1}{p}} \geq \widehat{L}_p(\bar{R}(X), \bar{R}(Y))$, where $c = \max\{\widehat{R}_{d_\infty}(X)(0), \widehat{R}_{d_\infty}(Y)(0)\}$.

The hierarchical stabilization process along a non-decreasing sequence of pseudometrics on T converts a discrete invariant $R: T \rightarrow \mathbf{N}$ into a stable invariant $\bar{R}: T \rightarrow \mathcal{M}_2$. We can now state our key definition:

Definition 2.3. Let T be a category with its set of objects also denoted by T . A sequence of pseudometrics $\{d_\alpha\}_{\alpha \in [0, \infty]}$ on T is called **ample** for $R: T \rightarrow \mathbf{N}$ if it is admissible for R , and the hierarchical stabilization $\bar{R}: T \rightarrow \mathcal{M}_2$ along this sequence has the following property: X and Y in T are isomorphic if and only if $\bar{R}(X) = \bar{R}(Y)$.

Let T be a category. By definition ample for $R: T \rightarrow \mathbf{N}$ sequences of pseudometrics on T lead to stable embeddings of isomorphism classes of objects in T into \mathcal{M}_2 . By choosing such an embedding, we can think about T as a subspace of \mathcal{M}_2 in which rich probability and statistical methods are well developed. Different sequences which are ample for R give different embeddings. Our expectation is that by choosing an appropriate such embedding, structural properties of T relevant to a data analysis task could be reflected by the geometry of the image of \bar{R} in \mathcal{M}_2 described by the L_p or interleaving metrics. The focus of this article is on T being the category $\text{Tame}([0, \infty), \text{Vec}_K)$ of tame $[0, \infty)$ -parametrized K vector spaces (also called one parameter tame persistence modules) and $R: \text{Tame}([0, \infty), \text{Vec}_K) \rightarrow \mathbf{N}$ being the minimal number of generators or equivalently the number of bars in the bar decomposition.

3 Formal homological persistence

A typical input for persistent homology is a collection $\{(X_i, d_i)\}$ of finite pseudometric spaces. Since homological persistence is about looking for homological features, each element of such data needs to be transformed into an object

reflecting these features more directly. The first step in this transformation is to convert the metric information into a simplicial complex parametrized by the poset $[0, \infty)$ whose elements are referred to as scales in this context. In this paper the Vietoris-Rips construction is used for that purpose, which at a scale $a \in [0, \infty)$ is a simplicial complex $\text{VR}_a(X_i, d_i)$ whose k -simplices are subsets of X_i consisting of $k + 1$ points which are pairwise at most distance a from each other. For example, two elements p_1 and p_2 in X_i connect to an edge, or a 1-simplex, when $d_i(p_1, p_2) \leq a$. If $a \leq b$, then $\text{VR}_a(X_i, d_i) \subseteq \text{VR}_b(X_i, d_i)$. The obtained filtration indexed by the poset $[0, \infty)$ is denoted by the symbol $\text{VR}(X_i, d_i)$.

Note that $\text{VR}(X_i, d_i)$ does not add or forget any information about (X_i, d_i) and hence is as complicated as the metric space itself. Simplification is therefore necessary and this is the purpose of the second step in this transformation in which the n -th homology (with coefficients in a chosen field K) is applied to the simplicial complexes in the Vietoris-Rips filtration. This results in a functor $H_n(\text{VR}(X_i, d_i), K): [0, \infty) \rightarrow \text{Vec}_K$ given by the linear functions $H_n(\text{VR}_a(X_i, d_i), K) \rightarrow H_n(\text{VR}_b(X_i, d_i), K)$ induced by the inclusions $\text{VR}_a(X_i, d_i) \subseteq \text{VR}_b(X_i, d_i)$ for $a \leq b$ in $[0, \infty)$. A functor of the form $V: [0, \infty) \rightarrow \text{Vec}_K$ is also called a $[0, \infty)$ -**parametrized K vector space** and the linear function $V_{a \leq b}: V_a \rightarrow V_b$, for $a \leq b$ in $[0, \infty)$, is called a **transition function**.

The functor $H_n(\text{VR}(X_i, d_i), K)$ is not an arbitrary $[0, \infty)$ -parametrized K vector space. It satisfies additional two properties which follow from finiteness of X_i :

Definition 3.1. An $[0, \infty)$ -parametrized K vector space V is called **tame** if:

1. the vector space V_a is finite dimensional for every a in $[0, \infty)$,
2. there are finitely many $0 < t_0 < \dots < t_k$ in $[0, \infty)$ such that, for $a \leq b$ in $[0, \infty)$, a transition function $V_{a \leq b}: V_a \rightarrow V_b$ may fail to be an isomorphism only if $a < t_i \leq b$ for some i .

For example constant functors are tame, in particular the 0 functor. If X is finite, then, for any pseudometric d on X , the functor $H_n(\text{VR}(X, d), K)$ is also tame. The symbol $\text{Tame}([0, \infty), \text{Vec}_K)$ denotes the collection of tame $[0, \infty)$ -parametrized K vector spaces. We refer to the process of assigning to a finite metric space (X, d) a tame $[0, \infty)$ -parametrized K vector space as **formal persistence**, the prominent example being the homology of the Vietoris-Rips construction $H_n(\text{VR}(X, d), K)$.

4 The rank

We recall how to define, calculate, and interpret the rank of a tame $[0, \infty)$ -parametrized K vector space. These are standard known results, which are included since the rank is the key discrete invariant studied in this paper. The rank is the number of bars in a bar decomposition. However to calculate the rank one does not need a bar decomposition. Calculating the rank is a much easier task than describing a bar decomposition.

4.1 Rank of a parametrized vector space

Let V be in $\text{Tame}([0, \infty), \text{Vec}_K)$. Choose $0 < t_0 < \dots < t_k$ in $[0, \infty)$ such that $V_{a \leq b}$ can fail to be an isomorphism only if $a < t_i \leq b$ for some i . Set:

$$H_0(V) := V_0 \oplus \text{coker}(V_{0 < t_0}) \oplus \text{coker}(V_{t_0 < t_1}) \cdots \oplus \text{coker}(V_{t_{k-1} < t_k}).$$

The vector space $H_0(V)$ is finite dimensional and does not depend on the choice of the sequence $0 < t_0 < \dots < t_k$. Define:

$$\text{rank}(V) := \dim(H_0(V)).$$

If V and W are tame $[0, \infty)$ -parametrized K vector spaces, then their direct sum $V \oplus W$ is also tame and $H_0(V \oplus W)$ is isomorphic to $H_0(V) \oplus H_0(W)$. In particular $\text{rank}(V \oplus W) = \text{rank}(V) + \text{rank}(W)$. Furthermore $\text{rank}(V) = 0$ if and only if $V = 0$.

4.2 Maps of parametrized vector spaces

A map or a natural transformation between two $[0, \infty)$ -parametrized K vector spaces V and W , denoted by $f: V \rightarrow W$, is a sequence $\{f_a: V_a \rightarrow W_a\}_{a \in [0, \infty)}$ of linear maps for which the following diagram commutes for every $a \leq b$ in $[0, \infty)$:

$$\begin{array}{ccc} V_a & \xrightarrow{V_{a \leq b}} & V_b \\ f_a \downarrow & & \downarrow f_b \\ W_a & \xrightarrow{W_{a \leq b}} & W_b \end{array}$$

The set of natural transformations between V and W is denoted by $\text{Nat}(V, W)$. Tame $[0, \infty)$ -parametrized K vector spaces together with maps between them and the composition given by the parameter-wise composition is a category which is denoted also by $\text{Tame}([0, \infty), \text{Vec}_K)$. This is the only category structure we consider on the set $\text{Tame}([0, \infty), \text{Vec}_K)$. In this category $f: V \rightarrow W$ is an epimorphism, a monomorphism or an isomorphism if and only if, for every a , the linear function f_a is, respectively, an epimorphism, a monomorphism or an isomorphism of vector spaces.

4.3 Bars

Let $s < e$ be in $[0, \infty]$ (s for start and e for end). Note that e might be equal to ∞ . Define $K(s, e)$ to be the $[0, \infty)$ -parametrized K vector space given by:

$$K(s, e)_a = \begin{cases} K, & \text{if } s \leq a < e \\ 0, & \text{otherwise,} \end{cases}$$

$$K(s, e)_{a \leq b}: K(s, e)_a \rightarrow K(s, e)_b = \begin{cases} \text{id}, & \text{if } \dim K(s, e)_a = \dim K(s, e)_b = 1 \\ 0, & \text{otherwise.} \end{cases}$$

We call $K(s, e)$ the **bar starting in s and ending in e** . If $e < \infty$, then $K(s, e)$ is called **finite**. Note that $K(s, e)$ is tame and $\text{rank}(K(s, e)) = 1$.

Let s be in $[0, \infty)$ and V be a $[0, \infty)$ -parametrized K vector space. The function $\text{Nat}(K(s, \infty), V) \rightarrow V_s$, assigning to a map $f: K(s, \infty) \rightarrow V$ the element

$f_s(1)$ in V_s , is a bijection. Thus every element x in V_s yields a unique map denoted by the same symbol $x: K(s, \infty) \rightarrow V$ for which $x(1) = x$. Similarly a set of elements $\{g_i \in V_{s_i}\}_{1 \leq i \leq n}$ yields a unique map $[g_1 \cdots g_n]: \bigoplus_{i=1}^n K(s_i, \infty) \rightarrow V$. Its image is denoted by $\langle g_1 \cdots g_n \rangle$ and called the $[0, \infty)$ -parametrized K vector subspace of V **generated by** $\{g_i \in V_{s_i}\}_{1 \leq i \leq n}$. It is the smallest subspace of V containing all the g_i 's. If $\langle g_1 \cdots g_n \rangle = V$, then the set $\{g_i \in V_{s_i}\}_{1 \leq i \leq n}$ is said to **generate** V .

Assume $s < e < \infty$. Then the function $\text{Nat}(K(s, e), V) \rightarrow V_s$, assigning to a map $f: K(s, e) \rightarrow V$ the element $f_s(1)$ in V_s is an inclusion. Its image coincides with $\ker(V_{s \leq e}: V_s \rightarrow V_e)$. Thus every element x in $\ker(V_{s \leq e}: V_s \rightarrow V_e)$ yields a unique $f: K(s, e) \rightarrow V$ for which $f_s(1) = x$. This map is also denoted by the symbol x .

4.4 Monotonicity of the rank

Let V be in $\text{Tame}([0, \infty), \text{Vec}_K)$. For any choice of a finite set $\{g_i \in V_{s_i}\}_{1 \leq i \leq n}$, the subspace $\langle g_1 \cdots g_n \rangle$ is tame. Furthermore $\text{rank}(\langle g_1 \cdots g_n \rangle) \leq \text{rank}(V)$. We refer to this property as the **monotonicity of the rank**.

4.5 Rank and the number of generators

Let $f: V \rightarrow W$ be a map between tame $[0, \infty)$ -parametrized K vector spaces. Let $0 < t_0 < \cdots < t_k$ be in $[0, \infty)$ such that $V_{a \leq b}$ or $W_{a \leq b}$ can fail to be an isomorphism only if $a < t_i \leq b$ for some i . For every $i > 0$, there is a unique linear map $\bar{f}_i: \text{coker}(V_{t_{i-1} < t_i}) \rightarrow \text{coker}(W_{t_{i-1} < t_i})$ making the following diagram commutative:

$$\begin{array}{ccccc} V_{t_{i-1}} & \xrightarrow{V_{t_{i-1} < t_i}} & V_{t_i} & \longrightarrow & \text{coker}(V_{t_{i-1} < t_i}) \\ f_{t_{i-1}} \downarrow & & \downarrow f_{t_i} & & \downarrow \bar{f}_i \\ W_{t_{i-1}} & \xrightarrow{W_{t_{i-1} < t_i}} & W_{t_i} & \longrightarrow & \text{coker}(W_{t_{i-1} < t_i}) \end{array}$$

Define $H_0(f): H_0(V) \rightarrow H_0(W)$ to be $f_0 \oplus \bigoplus_{i=1}^k \bar{f}_i$. Again the map $H_0(f)$ does not depend on the choice of the sequence $0 < t_0 < \cdots < t_k$.

It turns out that $f: V \rightarrow W$ is an epimorphism if and only if $H_0(f): H_0(V) \rightarrow H_0(W)$ is surjective. This is the key observation that can be used to show that $\text{rank}(V)$ **coincides with the smallest number of elements generating** V . In particular tame $[0, \infty)$ -parametrized K vector spaces are finitely generated.

4.6 Ends of elements

Let V be a tame $[0, \infty)$ -parametrized K vector space. For $x \neq 0$ in V_s , consider $L(x) := \{t \in [s, \infty) \mid V_{s \leq t}(x) \neq 0\}$ and define **the end of** x to be $e(x) := \sup(L(x))$. Note that either $e(x) = \infty$ or $e(x) < \infty$ in which case tameness implies $V_{s \leq e(x)}(x) = 0$. The induced map $x: K(s, e(x)) \rightarrow V$ is a monomorphism.

4.7 Rank and the number of bars

Let V be a tame $[0, \infty)$ -parametrized K vector space. An element $x \neq 0$ in V_s is defined to **generate a bar in** V , if $x: K(s, e(x)) \rightarrow V$ has a retraction, i.e., a map

$r: V \rightarrow K(s, e(x))$ for which the following composition is the identity:

$$\begin{array}{ccccc} K(s, e(x)) & \xrightarrow{x} & V & \xrightarrow{r} & K(s, e(x)) \\ & & \searrow \text{id} & \nearrow & \end{array}$$

In this case $K(s, e(x))$ is a direct summand of V .

A sequence of elements $\{g_i \in V_{s_i}\}_{1 \leq i \leq n}$ is called a **sequence of bar generators** for V if the induced map $[g_1 \cdots g_n]: \bigoplus_{i=1}^n K(s_i, e(g_i)) \rightarrow V$ is an isomorphism. The fundamental structure theorem states that every tame $[0, \infty)$ -parametrized K vector space admits a sequence of bar generators. In particular every tame $[0, \infty)$ -parametrized K vector space is isomorphic to a direct sum of bars.

This structure theorem can be proven by induction on the rank. If $\text{rank}(V) = 0$, then the empty sequence is a sequence of bar generators. Let $\text{rank}(V) = n > 0$. Assume the statement is true if the rank is smaller than n . Let $\{x_i \in V_{s_i}\}_{1 \leq i \leq n}$ be a set of generators of V . Set $l := \max\{e(x_1) - s_1, \dots, e(x_n) - s_n\}$. Among $\{x_i \mid e(x_i) - s_i = l\}$ choose x_j for which $e(x_j)$ is the largest. We claim that x_j generates a bar. This implies that V is isomorphic to $K(s_j, e(x_j)) \oplus W$. Thus $\text{rank}(W) = n - 1$ and by induction W admits a sequence of bar generators.

The discrete invariant we focus on in this paper is the rank or equivalently the minimal number of generators, or the number of bar generators:

$$\text{rank}: \text{Tame}([0, \infty), \text{Vec}_K) \rightarrow \mathbf{N}.$$

Our aim is to study its hierarchical stabilizations as explained in Section 2. For that we need to produce pseudometrics on $\text{Tame}([0, \infty), \text{Vec}_K)$. Noise systems in [17] were introduced exactly for this purpose. For implementing on a computer so called simple noise systems [7, Definition 8.2] are more convenient. The reason is that simple noise systems are parametrized by **contours** [7, Theorem 9.6]. Instead of explaining the theory behind noise systems, we focus in this article on discussing only contours and how they can directly be used to define pseudometrics on $\text{Tame}([0, \infty), \text{Vec}_K)$. Contours are also effective in calculating induced hierarchical stabilizations of the rank. We believe however that it is important to be aware of the relation between contours and noise systems.

5 Contours

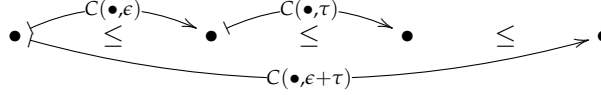
Definition 5.1. A **contour** is a function $C: [0, \infty] \times [0, \infty) \rightarrow [0, \infty]$ satisfying the following inequalities for all a and b in $[0, \infty]$ and ϵ and τ in $[0, \infty)$:

1. if $a \leq b$ and $\epsilon \leq \tau$, then $C(a, \epsilon) \leq C(b, \tau)$;
2. $a \leq C(a, \epsilon)$;
3. $C(C(a, \epsilon), \tau) \leq C(a, \epsilon + \tau)$.

Let C be a contour. C is an **action** if $C(a, 0) = a$ and $C(C(a, \tau), \epsilon) = C(a, \tau + \epsilon)$ for all a in $[0, \infty]$ and τ and ϵ in $[0, \infty)$. C is **closed** if the set $\{\epsilon \in [0, \infty) \mid C(a, \epsilon) \geq b\}$ is closed for all $a < b$ in $[0, \infty]$. C is **regular** if the following conditions are satisfied:

- $C(-, \epsilon): [0, \infty] \rightarrow [0, \infty]$ is a monomorphism for every ϵ in $[0, \infty)$,
- $C(a, -): [0, \infty) \rightarrow [0, \infty]$ is a monomorphism whose image is $[a, \infty)$ for every a in $[0, \infty)$.

The first condition of 5.1 makes sure that a contour preserves the poset structures. The second and third one can be depicted graphically as:



If C is a regular contour, then for $a < b$ in $[0, \infty]$:

$$\{\epsilon \in [0, \infty) \mid C(a, \epsilon) \geq b\} = \begin{cases} \{\epsilon \in [0, \infty) \mid \epsilon \geq C(a, -)^{-1}(b)\}, & \text{if } a < b < \infty \\ \emptyset, & \text{if } a < b = \infty. \end{cases}$$

Since all the sets on the right above are closed, regular contours are therefore closed. For contours to be useful as tools in data analysis we need methods to produce them. We now present several of them along with examples.

Definition 5.1 gives three functional inequalities implicitly characterizing contours. The last inequality however makes it difficult to give explicit formulas. We can in any case make initial guesses for the form of a contour and then try to find a formula satisfying the requirements of Definition 5.1.

5.2 Exponential contours

Let $f: [0, \infty) \rightarrow [0, \infty)$ be a non-decreasing function such that $f(0) \geq 1$. For (a, ϵ) in $[0, \infty] \times [0, \infty)$, define $C(a, \epsilon) := f(\epsilon)a$. Then C satisfies the first two inequalities of 5.1. The third inequality is equivalent to:

$$C(C(a, \epsilon), \tau) = C(f(\epsilon)a, \tau) = f(\tau)f(\epsilon)a \leq f(\epsilon + \tau)a = C(a, \epsilon + \tau).$$

For instance, since $e^\tau e^\epsilon = e^{\epsilon + \tau}$, the function C associated with the exponential function e^x is a contour. In fact we could choose any positive base number r other than e . Such contours are called **exponential**. Exponential contours are actions.

5.3 Standard contour

Let $f: [0, \infty) \rightarrow [0, \infty)$ be a non-decreasing function. For (a, ϵ) in $[0, \infty] \times [0, \infty)$, define $C(a, \epsilon) := a + f(\epsilon)$. Then C satisfies the first two inequalities of 5.1. The third inequality is equivalent to $a + f(\epsilon) + f(\tau) \leq a + f(\epsilon + \tau)$. Thus for C to be a contour, f should be superlinear: $f(\epsilon) + f(\tau) \leq f(\epsilon + \tau)$. For example $C(a, \epsilon) = a + \epsilon$ is a contour called the **standard contour**. The standard contour is an action which is regular. Another example is the **parabolic contour** $C(a, \epsilon) = a + \epsilon^2$. The parabolic contour is not an action, however it is regular. In fact all contours of the form $C(a, \epsilon) = a + f(\epsilon)$ are regular if f is superlinear and strictly increasing.

Contours can also be described by integral equations. In Sections 5.4 and 5.5 we consider a Lebesgue measurable function $f: [0, \infty) \rightarrow (0, \infty)$ with strictly positive values referred to as a **density**. In Section 10 we illustrate visualizations of some densities and the associated contours of the following two types.

5.4 Contours of distance type

Since f has strictly positive values, for (a, ϵ) in $[0, \infty) \times [0, \infty)$, there is a unique $D_f(a, \epsilon)$ in $[a, \infty)$ for which:

$$\epsilon = \int_a^{D_f(a, \epsilon)} f(x) dx.$$

Additivity of integrals gives for ϵ and τ in $[0, \infty)$:

$$\epsilon + \tau = \int_a^{D_f(a, \epsilon)} f(x) dx + \int_{D_f(a, \epsilon)}^{D_f(D_f(a, \epsilon), \tau)} f(x) dx = \int_a^{D_f(D_f(a, \epsilon), \tau)} f(x) dx$$

implying $D_f(D_f(a, \epsilon), \tau) = D_f(a, \epsilon + \tau)$. The inequality $D_f(a, \epsilon) \leq D_f(b, \tau)$, for $a \leq b < \infty$ and $\epsilon \leq \tau < \infty$, is a consequence of the monotonicity of integrals. If in addition we set $D_f(\infty, \epsilon) := \infty$, then the obtained function $D_f: [0, \infty) \times [0, \infty) \rightarrow [0, \infty]$ is a contour, even an action. It is called of **distance type** as it describes the distance needed to move from a to the right in order for the area under the graph of f to reach ϵ . Distance type contours are regular. If density is the constant function 1, then $\epsilon = \int_a^{D_1(a, \epsilon)} dx = D_1(a, \epsilon) - a$ and thus $D_1(a, \epsilon) = a + \epsilon$ is the standard contour (see 5.3).

5.5 Contours of shift type

For a in $[0, \infty]$, there is a unique y in $[0, \infty]$ such that $a = \int_0^y f(x) dx$. Define:

$$S_f(a, \epsilon) := \int_0^{y+\epsilon} f(x) dx.$$

Monotonicity of integrals implies that S_f satisfies the first two inequalities of Definition 5.1. Since $a = \int_0^y f(x) dx$ and $S_f(a, \epsilon) = \int_0^{y+\epsilon} f(x) dx$, by definition:

$$S_f(S_f(a, \epsilon), \tau) = \int_0^{y+\epsilon+\tau} f(x) dx = S_f(a, \epsilon + \tau).$$

The function S_f is therefore a contour which is an action. By writing $S_f(a, \epsilon) = a + \int_y^{y+\epsilon} f(x) dx$ for $a = \int_0^y f(x) dx$, we see S_f is a translation of a by the ϵ -step integral of the density. Therefore it is called of **shift type**. Shift type contours are regular. If the density is the constant function 1, then $a = \int_0^a dx$ and hence $S_1(a, \epsilon) = \int_0^{a+\epsilon} dx = a + \epsilon$ is the standard contour.

5.6 Truncating contours

Let $C: [0, \infty) \times [0, \infty) \rightarrow [0, \infty]$ be a contour. Choose an element α in $[0, \infty]$. For (a, ϵ) in $[0, \infty) \times [0, \infty)$ define:

$$(C/\alpha)(a, \epsilon) := \begin{cases} C(a, \epsilon), & \text{if } C(a, \epsilon) < \alpha \\ \infty, & \text{if } C(a, \epsilon) \geq \alpha. \end{cases}$$

For example $C/0 = \infty$ and $C/\infty = C$. We claim that C/α is a contour. The first two inequalities of Definition 5.1 are clear. It remains to show:

$$(C/\alpha)((C/\alpha)(a, \epsilon), \tau) \leq (C/\alpha)(a, \epsilon + \tau).$$

The inequality is clear if $C(a, \epsilon + \tau) \geq \alpha$. Assume $C(a, \epsilon + \tau) < \alpha$. This implies that also $C(a, \epsilon) < \alpha$ and $C(C(a, \epsilon), \tau) < \alpha$. Consequently $(C/\alpha)((C/\alpha)(a, \epsilon), \tau) = C(C(a, \epsilon), \tau)$ and $(C/\alpha)(a, \epsilon + \tau) = C(a, \epsilon + \tau)$ and hence in this case the inequality follows from the fact that C is a contour.

The contour C/α is called the **truncation** of C at α . If C is closed, then so is its truncation C/α for α in $[0, \infty]$. If $\alpha \leq \beta$ in $[0, \infty]$, then for (a, ϵ) in $[0, \infty] \times [0, \infty)$:

$$\infty = (C/0)(a, \epsilon) \geq (C/\alpha)(a, \epsilon) \geq (C/\beta)(a, \epsilon) \geq C(a, \epsilon).$$

5.7 Almost a contour

Let $C : [0, \infty] \times [0, \infty) \rightarrow [0, \infty]$ be a contour. Choose an element α in $[0, \infty]$. For (a, ϵ) in $[0, \infty] \times [0, \infty)$ define:

$$(C//\alpha)(a, \epsilon) := \begin{cases} \infty, & \text{if } a = \infty \\ C(a, \epsilon), & \text{if } a < \infty \text{ and } C(a, \epsilon) - a < \alpha \\ \infty, & \text{if } a < \infty \text{ and } C(a, \epsilon) - a \geq \alpha. \end{cases}$$

Is the function $(C//\alpha)$ a contour? The second inequality of Definition 5.1 is clear. The third inequality $(C//\alpha)((C//\alpha)(a, \epsilon), \tau) \leq (C//\alpha)(a, \epsilon + \tau)$ is clear if $a = \infty$ or $a < \infty$ and $C(a, \epsilon + \tau) - a \geq \alpha$. Assume $a < \infty$ and $C(a, \epsilon + \tau) - a < \alpha$. This implies:

$$\begin{aligned} C(a, \epsilon) - a &\leq C(a, \epsilon + \tau) - a < \alpha, \\ C(C(a, \epsilon), \tau) - C(a, \epsilon) &\leq C(a, \epsilon + \tau) - a < \alpha. \end{aligned}$$

Thus $(C//\alpha)((C//\alpha)(a, \epsilon), \tau) = C(C(a, \epsilon), \tau)$ and $(C//\alpha)(a, \epsilon + \tau) = C(a, \epsilon + \tau)$. The desired inequality follows from the fact that C is a contour.

If $\epsilon \leq \tau$, then since $C(a, \epsilon) - a \leq C(a, \tau) - a$, the inequality $(C//\alpha)(a, \epsilon) \leq (C//\alpha)(a, \tau)$ holds for any a . Thus the function $C//\alpha$ satisfies almost all of the requirements of the Definition 5.1 except possibly for the preservation of the poset relation in the first variable. This last requirement can in fact fail to be satisfied. For example consider the distance contour D_f with respect to the density given in Figure 7. In this case $D_f(0.2, 1) - 0.2 > 1.7$ and $D_f(0.3, 1) - 0.3 < 1.7$. Thus $(D_f//1.7)(0.2, 1) = \infty$ and $(D_f//1.7)(0.3, 1) = D_f(0.3, 1) < 2$.

It turns out that all the results in this article regarding contours until Theorem 7.1 do not require the assumption of the preservation of the poset relation in the first variable. Exploring generalizations of contours to functions that do not preserve order in the first variable is a part of our current research.

Contours appeared independently in [5] under the name superlinear families where they were used to define interleaving distances between generalized persistence modules. Since then generalized persistence modules have gathered some interest, see [11] and [15]. In this section we presented a variety of ways of constructing contours greatly enlarging [5], in which only

the standard contour is given as a concrete example of a superlinear family. The aim of the next section is to show how contours lead to pseudometrics on $\text{Tame}([0, \infty), \text{Vec}_K)$.

6 Constructing pseudometrics from contours

In this section we explain how to use a contour to define a pseudometric on $\text{Tame}([0, \infty), \text{Vec}_K)$. The initial idea developed together with Oliver Gäfvert and some of the text and diagrams below were written by him. It is also planned for some of this material to be a part of Oliver's future work. We refer to the thesis work [6] and paper [7] for relevant background that lead us together with Oliver to discover this connection between contours and pseudometrics.

To estimate how far apart tame parametrized vector spaces are from each other with respect to a contour we use the notion of equivalences:

Definition 6.1. Let $C: [0, \infty) \times [0, \infty) \rightarrow [0, \infty]$ be a contour, V and W be tame $[0, \infty)$ -parametrized K vector spaces, and ϵ be in $[0, \infty)$.

1. A map $f: V \rightarrow W$ is called an ϵ -**equivalence** (with respect to C) if, for every a in $[0, \infty)$ such that $C(a, \epsilon) < \infty$, there is a linear function $W_a \rightarrow V_{C(a, \epsilon)}$ making the following diagram commutative:

$$\begin{array}{ccc} V_a & \xrightarrow{V_{a \leq C(a, \epsilon)}} & V_{C(a, \epsilon)} \\ f_a \downarrow & \nearrow & \downarrow f_{C(a, \epsilon)} \\ W_a & \xrightarrow{W_{a \leq C(a, \epsilon)}} & W_{C(a, \epsilon)} \end{array}$$

2. The objects V and W are called ϵ -**equivalent** (with respect to C) if there is a tame $[0, \infty)$ -parametrized K vector space X and maps $f: V \rightarrow X \leftarrow W: g$ such that f is an ϵ_1 -equivalence, g is an ϵ_2 -equivalence, and $\epsilon_1 + \epsilon_2 \leq \epsilon$.
3. Let $S := \{\epsilon \in [0, \infty) \mid V \text{ and } W \text{ are } \epsilon\text{-equivalent}\}$. Define:

$$d_C(V, W) := \begin{cases} \infty, & \text{if } S = \emptyset \\ \inf(S), & \text{if } S \neq \emptyset. \end{cases}$$

If $C = \infty$, then every map is a 0-equivalence, all tame $[0, \infty)$ -parametrized K vector spaces V and W are 0-equivalent, and $d_C(V, W) = 0$. A monomorphism $f: V \rightarrow W$ in $\text{Tame}([0, \infty), \text{Vec}_K)$ is an ϵ -equivalence with respect to C if and only if the image of $W_{a \leq C(a, \epsilon)}: W_a \rightarrow W_{C(a, \epsilon)}$ is included in the image of $f_{C(a, \epsilon)}: V_{C(a, \epsilon)} \rightarrow W_{C(a, \epsilon)}$ for all a in $[0, \infty)$ such that $C(a, \epsilon) < \infty$. In particular $0 \rightarrow W$ is an ϵ -equivalence if and only if $W_{a \leq C(a, \epsilon)}: W_a \rightarrow W_{C(a, \epsilon)}$ is the zero function for all such a . Furthermore W is ϵ -equivalent to 0 if and only if $0 \rightarrow W$ is an ϵ -equivalence. Thus $d_C(0, W) < \epsilon$ if and only if $W_{a \leq C(a, \epsilon)}: W_a \rightarrow W_{C(a, \epsilon)}$ is the zero function for all a in $[0, \infty)$ such that $C(a, \epsilon) < \infty$. It is however not true in general that if $\epsilon = d_C(0, W) < \infty$, then $W_{a \leq C(a, \epsilon)}: W_a \rightarrow W_{C(a, \epsilon)}$ is the zero function for a in $[0, \infty)$ such that $C(a, \epsilon) < \infty$. This depends if C is closed or not.

According to Definition 6.1, to estimate and calculate $d_C(V, W)$, the objects V and W are compared through a third tame $[0, \infty)$ -parametrized vector space via a short zig-zag of equivalences $V \rightarrow X \leftarrow W$. In principal to assure the triangular inequality and obtain a pseudometric one should compare V and W not via short but long zig-zags $V \rightarrow X_0 \leftarrow \cdots \rightarrow X_k \rightarrow W$ of equivalences. The main content of the next proposition is that in our case short zig-zags are sufficient.

Proposition 6.1. d_C is a pseudometric on $\text{Tame}([0, \infty), \text{Vec}_K)$.

To prove this proposition and explain why short zig-zags are sufficient we need:

Proposition 6.2. Let $C: [0, \infty] \times [0, \infty) \rightarrow [0, \infty]$ be a contour and U, V , and W be tame $[0, \infty)$ -parametrized K vector spaces.

1. Composition of τ - and ϵ -equivalences is an $(\tau + \epsilon)$ -equivalence.
2. In the following pushout square, P is also tame and, if f is an ϵ -equivalence, then so is g :

$$\begin{array}{ccc} V & \longrightarrow & U \\ f \downarrow & & \downarrow g \\ W & \longrightarrow & P \end{array}$$

Proof. (1): Consider an ϵ -equivalence $g: U \rightarrow V$ and a τ -equivalence $f: V \rightarrow W$. If $C(a, \tau + \epsilon) < \infty$, then $C(a, \tau) \leq C(C(a, \tau), \epsilon) \leq C(a, \tau + \epsilon) < \infty$ and hence, for any such a , there are linear functions $W_a \rightarrow V_{C(a, \tau)} \rightarrow U_{C(C(a, \tau), \epsilon)}$ making the following diagram commutative:

$$\begin{array}{ccccccc} U_a & \longrightarrow & U_{C(a, \tau)} & \longrightarrow & U_{C(C(a, \tau), \epsilon)} & \longrightarrow & U_{C(a, \tau + \epsilon)} \\ g_a \downarrow & & \downarrow & \nearrow & \downarrow & & \downarrow \\ V_a & \longrightarrow & V_{C(a, \tau)} & \longrightarrow & V_{C(C(a, \tau), \epsilon)} & \longrightarrow & V_{C(a, \tau + \epsilon)} \\ f_a \downarrow & \nearrow & \downarrow & & \downarrow & & \downarrow \\ W_a & \longrightarrow & W_{C(a, \tau)} & \longrightarrow & W_{C(C(a, \tau), \epsilon)} & \longrightarrow & W_{C(a, \tau + \epsilon)} \end{array}$$

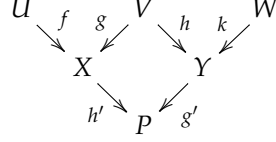
The diagonal morphism $W_a \rightarrow U_{C(a, \tau + \epsilon)}$ in this diagram is a linear function whose existence is required for fg to be an $(\tau + \epsilon)$ -equivalence.

(2): Tameness of P is clear. Assume $C(a, \epsilon) < \infty$. Let $W_a \rightarrow V_{C(a, \epsilon)}$ be a function given by the fact that $f: V \rightarrow W$ is an ϵ -equivalence. This function fits into the following cube where the dotted arrow is the unique function making this cube commutative (its existence is guaranteed by the universal property of push-outs):

$$\begin{array}{ccccc} V_a & \xrightarrow{\quad} & U_a & & \\ \downarrow f_a & \searrow & \downarrow g_a & \searrow & \\ & V_{C(a, \epsilon)} & \xrightarrow{\quad} & U_{C(a, \epsilon)} & \\ & \nearrow f_{C(a, \epsilon)} & \downarrow & \nearrow g_{C(a, \epsilon)} & \\ W_a & \xrightarrow{\quad} & P_a & \xrightarrow{\quad} & P_{C(a, \epsilon)} \\ & \searrow & \downarrow & \searrow & \\ & W_{C(a, \epsilon)} & \xrightarrow{\quad} & P_{C(a, \epsilon)} & \end{array}$$

□

Proof of Proposition 6.1. Symmetry is clear. For the triangle inequality consider ϵ -equivalent U and V , and τ -equivalent V and W and form the following diagram:



where f is an ϵ_1 -equivalence, g is an ϵ_2 -equivalence, $\epsilon_1 + \epsilon_2 \leq \epsilon$, h is a τ_1 -equivalence, k is a τ_2 -equivalence, $\tau_1 + \tau_2 \leq \tau$, and the central square in this diagram is a push-out. According to 6.2.(2), g' is an ϵ_2 -equivalence and h' is a τ_1 -equivalence. Thus 6.2.(1) implies $h'f$ is a $(\tau_1 + \epsilon_1)$ -equivalence and $g'k$ is a $(\tau_2 + \epsilon_2)$ -equivalence. Since $\epsilon + \tau \geq \tau_1 + \epsilon_1 + \tau_2 + \epsilon_2$, we can conclude that U and W are $(\epsilon + \tau)$ -equivalent. The triangle inequality $d_C(U, W) \leq d_C(U, V) + d_C(V, W)$ follows. \square

We are interested in not just individual pseudometrics but also in their sequences, particularly the non-decreasing ones (see Definition 2.2). To produce such sequences of pseudometrics on $\text{Tame}([0, \infty], \text{Vec}_K)$ we use:

Proposition 6.3. *Assume C and D are contours such that $C \geq D$. Then:*

1. *An ϵ -equivalence with respect to D implies ϵ -equivalence with respect to C .*
2. $d_C(V, W) \leq d_D(V, W)$.

Proof. Statement (2) is a direct consequence of (1). To show (1), let $f: V \rightarrow W$ be an ϵ -equivalence with respect to D . If $C(a, \epsilon) < \infty$, then also $D(a, \epsilon) < \infty$, and hence we can form the following commutative diagram whose diagonal is the function assuring f is an ϵ -equivalence with respect to C :

$$\begin{array}{ccccc}
 V_a & \xrightarrow{V_{a \leq D(a, \epsilon)}} & V_{D(a, \epsilon)} & \xrightarrow{V_{D(a, \epsilon) \leq C(a, \epsilon)}} & V_{C(a, \epsilon)} \\
 f_a \downarrow & \nearrow & \downarrow f_{D(a, \epsilon)} & & \downarrow f_{C(a, \epsilon)} \\
 W_a & \xrightarrow{W_{a \leq D(a, \epsilon)}} & W_{D(a, \epsilon)} & \xrightarrow{W_{D(a, \epsilon) \leq C(a, \epsilon)}} & W_{C(a, \epsilon)}
 \end{array}$$

\square

7 Stable ranks

We are now ready to discuss our models for supervised persistence:

Definition 7.1. Let C be a contour and d_C be the associated pseudometric on $\text{Tame}([0, \infty), \text{Vec}_K)$ (see Proposition 6.1). The hierarchical stabilization (see Section 2) of the rank function $\text{rank}: \text{Tame}([0, \infty), \text{Vec}_K) \rightarrow \mathbf{N}$ (see Section 4), with respect to d_C , is called **stable rank** and is denoted by:

$$\widehat{\text{rank}}_C: \text{Tame}([0, \infty), \text{Vec}_K) \rightarrow \mathcal{M}.$$

By Definition 2.1, the stable rank assigns to a tame $[0, \infty)$ -parametrized K vector space V , the function $\widehat{\text{rank}}_C V: [0, \infty) \rightarrow [0, \infty)$ defined as follows:

$$\widehat{\text{rank}}_C V(t) = \min \{ \text{rank}(W) \mid W \in \text{Tame}([0, \infty), \text{Vec}_K) \text{ and } d_C(V, W) \leq t \}.$$

Thus $\widehat{\text{rank}}_C V$ is non-increasing with natural numbers as values and therefore there are finitely many elements $0 < \tau_0 < \dots < \tau_n$ in its domain $[0, \infty)$ such that $\widehat{\text{rank}}_C V$ is constant on the open intervals $(0, \tau_0), \dots, (\tau_i, \tau_{i+1}), \dots, (\tau_n, \infty)$. Depending on the contour, $\widehat{\text{rank}}_C V$ may fail to be right or left continuous.

The aim of this section is to provide effective ways of calculating the stable rank. If a contour is closed (see Definition 5.1), then the following fundamental properties of the stable rank explain how its values are related to a bar decomposition. One can then use for example the Ripser software [1] for effective calculations of the stable rank.

Theorem 7.1. *If C is a closed contour, then $\widehat{\text{rank}}_C: \text{Tame}([0, \infty), \text{Vec}_K) \rightarrow \mathcal{M}$ satisfies the following properties:*

1. *The function $\widehat{\text{rank}}_C(V): [0, \infty) \rightarrow [0, \infty)$ is right continuous for any V .*
2. *The function $\widehat{\text{rank}}_C$ is linear: $\widehat{\text{rank}}_C(V \oplus W) = \widehat{\text{rank}}_C(V) + \widehat{\text{rank}}_C(W)$.*
3. *$\widehat{\text{rank}}_C(\bigoplus_{i=1}^n K(s_i, e_i))(t) = |\{i \mid C(s_i, t) < e_i\}|$.*

According to the third statement of Theorem 7.1, the values of the stable rank are certain counts of bars in a bar decomposition. Note that in our entire set up of the hierarchical stabilization process and in the definition of the stable rank no bar decomposition is mentioned or used. The aim of the hierarchical stabilization is to convert discrete invariants into stable invariants by minimizing over discs. The stable rank therefore encodes in a stable way some information about how ranks of tame $[0, \infty)$ -parametrized vector spaces change in certain neighbourhoods. Achieving stability is the key objective of this process. The linearity property (Theorem 7.1.(2)) is then what connects the stable rank with bar decompositions. Traditionally, in persistent homology one considers bar decompositions first and then proves that with respect to certain metrics the associated persistence diagrams are stable. The reversal of this perspective, **stability first and decompositions after**, has been an important step in our approach to homological persistence. Stability is so fundamental for any method aimed at data analysis that we believe it should be the primary guiding principle in homological persistence. Decompositions can be then used as effective tools for calculating the constructed stable invariants. This change of perspective is vital to multiparameter generalizations of homological persistence where decomposition methods are not available (see [7]).

Theorem 7.1 is a direct consequence of Corollary 7.6 and Proposition 7.2. This strategy to prove Theorem 7.1 is taken from [7] (see [7, Section 8]) and is based on:

Definition 7.2. Let C be a contour, t in $[0, \infty)$, and V in $\text{Tame}([0, \infty), \text{Vec}_K)$. The t -**shift** of V with respect to C , denoted by $V_C[t]$, is the $[0, \infty)$ -parametrized K vector subspace of V generated by all the elements in the images of the transition functions $V_{a \leq C(a, t)}: V_a \rightarrow V_{C(a, t)}$ for all a in $[0, \infty)$ such that $C(a, t) < \infty$.

The shift operation enjoys the following properties:

Proposition 7.2. *Let V, W be in $\text{Tame}([0, \infty), \text{Vec}_K)$, t in $[0, \infty)$, and C be a contour.*

1. *If V is generated by $\{g_i \in V_{s_i}\}_{1 \leq i \leq n}$, then $V_C[t]$ is generated by:*

$$\{V_{s_i \leq C(s_i, t)}(g_i) \mid 1 \leq i \leq n \text{ and } C(s_i, t) < \infty\}.$$

2. *$V_C[t]$ is tame.*

3. *The inclusion $V_C[t] \subset V$ is a t -equivalence with respect to C .*

4. *A monomorphism $f: W \subset V$ is a t -equivalence if and only if $V_C[t]$ is contained in the image of f .*

5. *The shift is linear: $(V \oplus W)_C[t]$ and $V_C[t] \oplus W_C[t]$ are isomorphic.*

6. *$(\bigoplus_{i=1}^n K(s_i, e_i))_C[t]$ is isomorphic to $\bigoplus_{\{i \mid C(s_i, t) < e_i\}} K(C(s_i, t), e_i)$.*

7. *$\text{rank}((\bigoplus_{i=1}^n K(s_i, e_i))_C[t]) = |\{i \mid C(s_i, t) < e_i\}|$.*

Proof. (1) is a direct consequence of the definitions; (2), (3), (4), (5), and (6) follow from (1), and (7) from (6). \square

If $t \leq t'$ in $[0, \infty)$, then $V_C[t] \supset V_C[t']$ and therefore by the monotonicity of rank (see 4.4), $\text{rank}(V_C[t]) \geq \text{rank}(V_C[t'])$. Thus the function $t \mapsto \text{rank}(V_C[t])$ is non-increasing and, similarly to the stable rank, there are finitely many elements $0 < \tau_0 < \dots < \tau_n$ in $[0, \infty)$ such that $\text{rank}(V_C[-])$ is constant on the open intervals $(0, \tau_0), \dots, (\tau_i, \tau_{i+1}), \dots, (\tau_n, \infty)$.

Proposition 7.3. *Let V be a tame $[0, \infty)$ -parametrized K vector space. If C is a closed contour, then $\text{rank}(V_C[-])$ is a right continuous function, i.e., there are finitely many $0 < \tau_0 < \dots < \tau_n$ in $[0, \infty)$ such that $\text{rank}(V_C[-])$ is constant on the left closed and right open intervals $[0, \tau_0), \dots, [\tau_i, \tau_{i+1}), \dots, [\tau_n, \infty)$.*

Proof. It is enough to show that for any t , there is $t < t'$ for which $\text{rank}(V_C[t]) = \text{rank}(V_C[t'])$. Let $0 < t_0 < \dots < t_k$ be such that $V_{a \leq b}: V_a \rightarrow V_b$ may fail to be an isomorphism only if $a < t_i \leq b$ for some i . Choose a sequence $\{g_i \in V_{s_i}\}_{1 \leq i \leq n}$ of generators of V . Consider only these $C(s_i, t)$ which lie in $[0, \infty)$. Since C is closed, there are $t < t'$ for which both $C(s_i, t)$ and $C(s_i, t')$ are in one of the intervals $[0, t_0), \dots, [t_n, \infty)$. Consequently the transition functions $V_{C(s_i, t) \leq C(s_i, t')}$, for all i , are isomorphisms and $V_C[t]$ and $V_C[t']$ have the same rank. \square

Here is the key relation between the stable rank and the shift operation:

Theorem 7.4. *Let C be a contour and V be in $\text{Tame}([0, \infty), \text{Vec}_K)$. Then for $t < t'$ in $[0, \infty)$:*

$$\text{rank}(V_C[t]) \geq \widehat{\text{rank}}_C(V)(t) \geq \text{rank}(V_C[t']).$$

Proof. Since $V_C[t] \subset V$ is a t -equivalence (see Proposition 7.2.(3)), $d_C(V, V_C[t]) \leq t$. This gives the first inequality.

Let W be a tame $[0, \infty)$ -parametrized K vector space for which $d_C(V, W) \leq t$ and $\text{rank}(W) = \widehat{\text{rank}}_C V(t)$. Since $d_C(V, W) < t'$, by definition there are maps

$f: V \rightarrow X \leftarrow W : g$ in $\text{Tame}([0, \infty), \text{Vec}_K)$ where f is τ_1 -equivalence, g is τ_2 -equivalence, and $\tau_1 + \tau_2 < t'$. For any a in $[0, \infty)$ such that $C(a, \tau_1) < \infty$, consider the following commutative diagram where the vertical arrows are the transition functions and β_a is the lift given by the fact that f is τ_1 -equivalence:

$$\begin{array}{ccccc} V_a & \xrightarrow{f} & X_a & \xleftarrow{g} & W_a \\ \downarrow & \nearrow \beta_a & \downarrow & & \downarrow \\ V_{C(a, \tau_1)} & \xrightarrow{f} & X_{C(a, \tau_1)} & \xleftarrow{g} & W_{C(a, \tau_1)} \end{array}$$

Let $n = \text{rank}(W)$ and $\{w_i \in W_{s_i}\}_{1 \leq i \leq n}$ be a minimal set of generators of W . Set $x_i := g(w_i)$. For any i in the set $I := \{i \mid C(s_i, \tau_1) < \infty\}$, define $v_i := \beta_{s_i}(g(w_i)) \in V_{C(s_i, \tau_1)}$ and $V' := \langle v_i \mid i \in I \rangle \subset V$. We claim that the following inclusions hold:

$$V_C[t'] \subset V_C[\tau_1 + \tau_2] \subset V' \subset V,$$

which imply $\widehat{\text{rank}}_C V(t) = n \geq \text{rank}(V') \geq \text{rank}(V_C[t'])$, proving the second inequality. The first inclusion is a consequence of $\tau_1 + \tau_2 < t'$. The last inclusion is by definition. It remains to show the middle inclusion $V_C[\tau_1 + \tau_2] \subset V'$.

For any a in $[0, \infty)$ such that $C(a, \tau_1 + \tau_2) < \infty$ we have the following commutative diagram where all the horizontal arrows indicate the transition functions, vertical arrows are functions induced by f and g , and $\beta_{C(a, \tau_2)}$ and α_a are lifts guaranteed by the fact that f is τ_1 -equivalence and g is τ_2 -equivalence, respectively:

$$\begin{array}{ccccccc} V_a & \longrightarrow & V_{C(a, \tau_2)} & \longrightarrow & V_{C(C(a, \tau_2), \tau_1)} & \longrightarrow & V_{C(a, \tau_1 + \tau_2)} \\ f_a \downarrow & & f \downarrow & \nearrow \beta_{C(a, \tau_2)} & \downarrow f & & \downarrow f \\ X_a & \longrightarrow & X_{C(a, \tau_2)} & \longrightarrow & X_{C(C(a, \tau_2), \tau_1)} & \longrightarrow & X_{C(a, \tau_1 + \tau_2)} \\ g_a \uparrow & \nwarrow \alpha_a & \uparrow g & & \uparrow g & & \uparrow g \\ W_a & \longrightarrow & W_{C(a, \tau_2)} & \longrightarrow & W_{C(C(a, \tau_2), \tau_1)} & \longrightarrow & W_{C(a, \tau_1 + \tau_2)} \end{array}$$

Commutativity of this diagram implies that, for every such a , the image of the transition function $V_{a \leq C(a, \tau_1 + \tau_2)}$ belongs to V' . Since $V_C[\tau_1 + \tau_2]$ is generated by these images, the inclusion $V_C[\tau_1 + \tau_2] \subset V'$ holds. \square

According to Theorem 7.4, the functions $\widehat{\text{rank}}_C(V)$ and $\text{rank}(V_C[-])$ agree for all but finitely many points:

Corollary 7.5. *Let C be a contour and V be in $\text{Tame}([0, \infty), \text{Vec}_K)$. Then there are $0 < \tau_0 < \dots < \tau_n$ in $[0, \infty)$ such that the functions $\widehat{\text{rank}}_C(V)$ and $\text{rank}(V_C[-])$ agree on the open intervals $(0, \tau_0), \dots, (\tau_i, \tau_{i+1}), \dots, (\tau_n, \infty)$. In particular, for $p \geq 1$:*

$$d_\infty(\widehat{\text{rank}}_C(V), \text{rank}(V_C[-])) = 0 = L_p(\widehat{\text{rank}}_C(V), \text{rank}(V_C[-])).$$

Theorem 7.4 together with Proposition 7.3 gives:

Corollary 7.6. *Assume C is a closed contour. Then $\widehat{\text{rank}}_C(V) = \text{rank}(V_C[-])$ for any V in $\text{Tame}([0, \infty), \text{Vec}_K)$.*

We finish this section with:

Corollary 7.7. *Assume C is a closed contour such that $C(a, 0) = a$ for any a in $[0, \infty]$. Let V be a tame $[0, \infty)$ -parametrized K vector space. Then:*

1. $\widehat{\text{rank}}_C V(0) = \text{rank}(V)$.
2. $\widehat{\text{rank}}_C V = 0$ if and only if $V = 0$.

Proof. Corollary 7.6 and Proposition 7.2.(1) imply $\widehat{\text{rank}}_C V(0) = \text{rank}(V_C[0]) = \text{rank}(V)$. Since $\widehat{\text{rank}}_C V$ is non-increasing, the identity $\widehat{\text{rank}}_C V = 0$ is equivalent to $\widehat{\text{rank}}_C V(0) = 0$, which by statement (1) is equivalent to $\text{rank}(V) = 0$, proving (2). \square

8 Life span

Let $s < e$ be in $[0, \infty]$. Since $\text{rank}(K(s, e)) = 1$, then, for a contour C , the value of $\widehat{\text{rank}}_C K(s, e)(t)$ is either 1 or 0. As the function $\widehat{\text{rank}}_C K(s, e)$ is non-increasing, there is l in $[0, \infty]$ such that:

$$\widehat{\text{rank}}_C K(s, e)(t) = \begin{cases} 1, & \text{if } t < l \\ 0, & \text{if } t > l. \end{cases}$$

We define $\text{life}_C K(s, e) := l$ and call this element in $[0, \infty]$ the **life span** of $K(s, e)$. If $l = \text{life}_C K(s, e) < \infty$, then the value $\widehat{\text{rank}}_C K(s, e)(l)$ can be either 1 or 0, depending on the contour. If C is closed, then according to Theorem 7.1.(1), $\widehat{\text{rank}}_C K(s, e)(l) = 0$. This with the additivity property in Theorem 7.1.(3) gives:

Proposition 8.1. *If C is a closed contour, then:*

$$\widehat{\text{rank}}_C \left(\bigoplus_{i=1}^n K(s_i, e_i) \right) (t) = |\{i \mid t < \text{life}_C K(s_i, e_i)\}|.$$

According to Proposition 8.1, the stable rank, with respect to a closed contour, counts bars whose life span strictly exceeds t . Here is how to calculate the life span for regular contours:

Proposition 8.2. *Let $s < e$ be in $[0, \infty]$ and α be in $[0, \infty)$. If C is a regular contour (see Definition 5.1), then:*

$$\begin{aligned} \text{life}_C K(s, e) &= \begin{cases} \infty, & \text{if } e = \infty \\ C(s, -)^{-1}(e), & \text{if } e < \infty, \end{cases} \\ \text{life}_{C/\alpha} K(s, e) &= \begin{cases} 0, & \text{if } \alpha \leq s \\ C(s, -)^{-1}(\alpha), & \text{if } s < \alpha \leq e \\ C(s, -)^{-1}(e), & \text{if } e < \alpha. \end{cases} \end{aligned}$$

Proof. According to Theorem 7.1.(3):

$$\widehat{\text{rank}}_C K(s, e)(t) = \begin{cases} 1, & \text{if } C(s, t) < e \\ 0, & \text{if } C(s, t) \geq e. \end{cases}$$

This together with the regularity of C implies all the claimed equalities. \square

Corollary 8.3. *If C is a regular contour, then:*

$$\lim \left(\widehat{\text{rank}}_C \left(\bigoplus_{i=1}^n K(s_i, e_i) \right) \right) = |\{i \mid e_i = \infty\}|.$$

9 Regular contours and ampleness

Let C be a contour. For every α in $[0, \infty]$, we can take its truncation C/α (see 5.6). In this way we get a sequence of contours indexed by $[0, \infty]$ such that for $\alpha < \beta$ in $[0, \infty]$:

$$\infty = C/0 \geq \dots \geq C/\alpha \geq \dots \geq C/\beta \geq \dots \geq C/\infty = C.$$

Each of these contours induces a pseudometric on $\text{Tame}([0, \infty), \text{Vec}_K)$ as defined in 6.1. In this way, according to Proposition 6.1, we obtain a sequence of pseudometrics $\{d_{C/\alpha}\}_{\alpha \in [0, \infty]}$. Furthermore, for all $\alpha < \beta$ in $[0, \infty]$ and V, W in $\text{Tame}([0, \infty), \text{Vec}_K)$, Proposition 6.3.(2) gives the following inequalities:

$$0 = d_{C/0}(V, W) \leq \dots \leq d_{C/\alpha}(V, W) \leq \dots \leq d_{C/\beta}(V, W) \leq \dots \leq d_C(V, W).$$

A contour therefore induces a non-decreasing sequence of pseudometrics on $\text{Tame}([0, \infty), \text{Vec}_K)$, leading to hierarchical stabilization (Definition 2.2.(4)):

$$\begin{array}{ccc} \text{Contours} & & \text{Tame}([0, \infty), \text{Vec}_K) \\ \downarrow \{d_{C/\alpha}\}_{\alpha \in [0, \infty]} & & \downarrow \overline{\text{rank}}_C \\ \text{Sequences of pseudometrics on } \text{Tame}([0, \infty), \text{Vec}_K) & & \mathcal{M}_2 \end{array}$$

We are now ready to state and prove our key ampleness result (see Definition 2.3 and discussion after):

Theorem 9.1. *Consider the category $\text{Tame}([0, \infty), \text{Vec}_K)$. If C is a regular contour, then the sequence of pseudometrics $\{d_{C/\alpha}\}_{\alpha \in [0, \infty]}$ is ample for the rank function $\text{rank}: \text{Tame}([0, \infty), \text{Vec}_K) \rightarrow \mathbf{N}$.*

Proof. Let V and W be tame $[0, \infty)$ -parametrized K vector spaces. Assume, for every α in $[0, \infty]$, $\widehat{\text{rank}}_{C/\alpha} V = \widehat{\text{rank}}_{C/\alpha} W$. We need to show V and W are isomorphic.

Since C is regular, then it is closed and $C(a, 0) = a$ for all a , and hence according to Corollaries 7.6 and 7.7:

$$\text{rank}(V) = \text{rank}(V_C[0]) = \widehat{\text{rank}}_C V(0) = \widehat{\text{rank}}_C W(0) = \text{rank}(W_C[0]) = \text{rank}(W).$$

Thus V and W have the same rank. Assume V is isomorphic to $\bigoplus_{i=1}^n K(s_i, e_i)$ and W is isomorphic to $\bigoplus_{i=1}^n K(s'_i, e'_i)$.

Step 1: Reduction to finite bars. According to Corollary 8.3:

$$|\{i \mid e_i = \infty\}| = \lim \left(\widehat{\text{rank}}_C V \right) = \lim \left(\widehat{\text{rank}}_C W \right) = |\{i \mid e'_i = \infty\}|.$$

Thus V and W are isomorphic to, respectively:

$$\bigoplus_{i=1}^{n_1} K(s_i, e_i) \oplus \bigoplus_{j=1}^{n_2} K(s_j, \infty) \quad \bigoplus_{i=1}^{n_1} K(s'_i, e'_i) \oplus \bigoplus_{j=1}^{n_2} K(s'_j, \infty),$$

where $e_i, e'_i < \infty$ for $i = 1, \dots, n_1$.

Choose β in $[0, \infty)$ such that $\beta > e_i, e'_i, s_j, s'_j$ for all i and j , and define:

$$V/\beta := \bigoplus_{i=1}^{n_1} K(s_i, e_i) \oplus \bigoplus_{j=1}^{n_2} K(s_j, \beta) \quad W/\beta := \bigoplus_{i=1}^{n_1} K(s'_i, e'_i) \oplus \bigoplus_{j=1}^{n_2} K(s'_j, \beta).$$

Note that V and W are isomorphic if and only if V/β and W/β are isomorphic. Thus to prove the theorem it is enough to show V/β and W/β are isomorphic.

We claim that, for every α in $[0, \infty]$, $\widehat{\text{rank}}_{C/\alpha}(V/\beta) = \widehat{\text{rank}}_{C/\alpha}(W/\beta)$. This follows from the assumption $\widehat{\text{rank}}_{C/\alpha} V = \widehat{\text{rank}}_{C/\alpha} W$, the additivity of the stable rank (Theorem 7.1.(2)), and Proposition 8.2 which gives that for all $s < \beta$:

$$\begin{aligned} \text{life}_{C/\alpha} K(s, \beta) &= C^{-1}(s, \alpha) = \text{life}_{C/\alpha} K(s, \infty), \quad \text{if } \alpha \leq \beta, \\ \text{life}_{C/\alpha} K(s, \beta) &= C^{-1}(s, \beta) = \text{life}_{C/\beta} K(s, \infty), \quad \text{if } \alpha > \beta. \end{aligned}$$

We reduced the theorem to the case when all the bars in the bar decompositions of V and W are finite.

Step 2: Induction on the rank. Assume V is isomorphic to $\bigoplus_{i=1}^n K(s_i, e_i)$ and W is isomorphic to $\bigoplus_{i=1}^n K(s'_i, e'_i)$ where $e_i, e'_i < \infty$. We are going to prove by induction on the rank that V and W are isomorphic. The statement is clear if $\text{rank}(V) = \text{rank}(W) = 0$, since in this case both V and W are isomorphic to 0. Assume $n = \text{rank}(V) > 0$. Let $l_i = \text{life}_C K(s_i, e_i)$ and $l'_i = \text{life}_C K(s'_i, e'_i)$ (see Section 8). Recall that according to Proposition 8.1, for t in $[0, \infty)$:

$$|\{i \mid t < l_i\}| = \widehat{\text{rank}}_C V(t) = \widehat{\text{rank}}_C W(t) = |\{i \mid t < l'_i\}|.$$

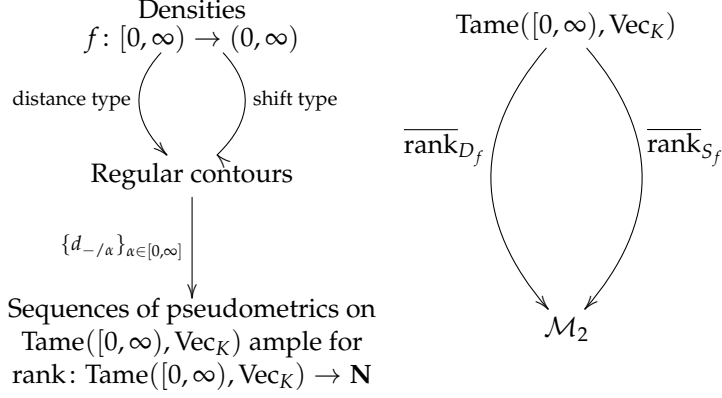
It follows that $l_{\max} := \max\{l_i \mid 1 \leq i \leq n\} = \max\{l'_i \mid 1 \leq i \leq n\}$. Let $e_{\max} := \max\{e_i \mid l_i = l_{\max}\}$ and $e'_{\max} := \max\{e'_i \mid l'_i = l_{\max}\}$. We claim that $e_{\max} = e'_{\max}$. If $e_{\max} < e'_{\max}$, then $\widehat{\text{rank}}_{C/e_{\max}} V > \widehat{\text{rank}}_{C/e_{\max}} W$ contradicting the assumption.

Since C is regular, there is a unique s such that $C(s, l_{\max}) = e_{\max}$. Thus both V and W contain the bar of the form $K(s, e_{\max})$ in their bar decompositions. We can then split off this bar and proceed by induction. \square

Corollary 9.2. *Tame $[0, \infty)$ -parametrized K vector spaces V and W are isomorphic if and only if $\widehat{\text{rank}}_C V = \widehat{\text{rank}}_C W$ for all contours C .*

Let us summarize our methods of producing embeddings of isomorphism classes of tame $[0, \infty)$ -parametrized K vector spaces into the space \mathcal{M}_2 of measurable functions of the form $[0, \infty)^2 \rightarrow [0, \infty)$. A density $f: [0, \infty) \rightarrow (0, \infty)$, which is a measurable function with strictly positive values, leads to two regular contours: the distance type D_f (see 5.4) and the shift type S_f (see 5.5). According to Theorem 9.1 each of these contours then leads to a sequence of

pseudometrics on $\text{Tame}([0, \infty), \text{Vec}_K)$ which is ample for the rank. In this way any density leads to embeddings illustrated in the following diagrams:



If the density is 1, then the distance and the shift type contours coincide and so do the induced embeddings. For other densities the contours and the embeddings are different. For example consider the constant densities 1 and 5, and the density f displayed in Figure 7. In Figure 1 we illustrate the following functions:

$$\begin{array}{l|l}
 D1 := \widehat{\text{rank}}_{D_1} V = \widehat{\text{rank}}_{S_1} V & Df/0.13 := \overline{\text{rank}}_{D_f} V(0.13, -) = \widehat{\text{rank}}_{D_f/0.13} V \\
 D5 := \widehat{\text{rank}}_{D_5} V & Df/0.3 := \overline{\text{rank}}_{D_f} V(0.3, -) = \widehat{\text{rank}}_{D_f/0.3} V \\
 S5 := \widehat{\text{rank}}_{S_5} V & Sf/0.13 := \overline{\text{rank}}_{S_f} V(0.13, -) = \widehat{\text{rank}}_{S_f/0.13} V \\
 & Sf/0.3 := \overline{\text{rank}}_{S_f} V(0.3, -) = \widehat{\text{rank}}_{S_f/0.3} V
 \end{array}$$

where V is a tame $[0, \infty)$ -parametrized vector space given by the first homology with \mathbf{F}_2 coefficients of the Vietoris-Rips construction on an IFS point process on a unit square as described in Section 10.2.

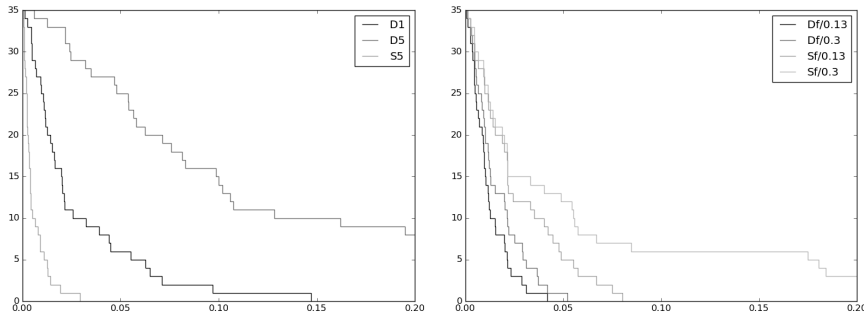


Figure 1: For densities different than 1, the embeddings described after Corollary 9.2 are different.

10 Using contours

In this section we illustrate how choosing a density and a contour can lead to improvements in classification results based on stable ranks. We emphasize that the focus is not on finding an optimal classifier for a specific case. The aim is to give concrete evidence to support our claim that the choice of metrics is fundamental in homological persistence and to explain how contours are used in concrete analysis. We also hope to convey that the presented theory leads to a practical TDA pipeline amenable particularly to machine learning. Further study of the efficacy of this pipeline and the choice of contours for particular tasks is the aim of ongoing research. Two case studies are considered, point processes on a unit square and real data from human activities. To generate bars needed for our calculations we used the Ripser software [1] with Vietoris-Rips filtration and homology with F_2 coefficients.

10.1 Visualizing bars and contours

The bars $K(s, e)$ of a $[0, \infty)$ -parametrized K vector space can be parametrized by the start s and the life span with respect to the standard contour C , $\text{life}_C K(s, e) = e - s$. Bars can then be visualized in an $(s, e - s)$ -plot as vertical stems. We call this presentation **stem plot**. For a reader accustomed to barcodes, the stem plot contains exactly the same information but plotted vertically. The horizontal axis is the filtration value and the vertical axis is the bar length. Taking into account multiplicity of more than one bar having the same start value we extend the domain of the stem plot to $[0, \infty) \times \mathbf{N}$, where \mathbf{N} is used to index bars with the same birth. However with real data this is needed basically only for the 0th homology since in the standard Vietoris-Rips filtration all the points and hence all the 0th homology classes are present at filtration value 0.

For a fixed t , the relation $C(s_i, t) < e_i$ in Theorem 7.1.(3) describes an area above the parametric curve $\gamma_t(s_i) = (s_i, C(s_i, t))$ in the (s, e) -plane. Setting $C(s_i, t) = e_i$ and applying the transformation $(s, e) \mapsto (s, e - s)$, we get a curve $\hat{\gamma}_t(s_i) = (s_i, C(s_i, t) - s_i)$. Such curves are typically called contour lines, hence the name contours.

Significance of stem plots comes when overlaid with contour lines. The right plot of Figure 2 illustrates a persistence stem plot along with contour lines of distance and shift contours for few values of t (dashed curves). Stem plot comes from one realization of point processes of Section 10.2. Density function used to calculate contours is also shown in the left plot. With contour lines the vertical axis of a stem plot corresponds to t in $C(s, t)$ and the horizontal axis is the filtration value s as explained above.

Stem plot and contour lines make it easy to understand visually Proposition 8.1: the value of the stable rank at t is the number of those bars that exceed the contour line at t . Thus on those regions where contour lines obtain low values, homological features are magnified and vice versa for larger values of contour lines. Stem plot can be an effective tool to gain understanding of stable ranks with respect to different contours and to explore appropriate ones for a given task.

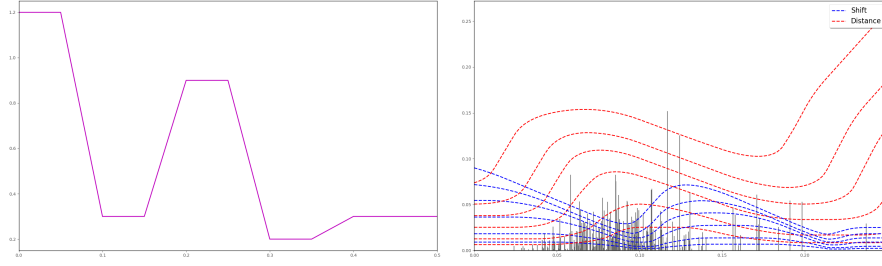


Figure 2: Distance and shift type contours visualized on a stem plot (right) with the same density function (left).

10.2 Point processes

Point processes have gathered interest in TDA community, see for example [4, 9, 16]. We simulated six different classes of point processes on a unit square, see their descriptions below. For each class we produced 500 simulations on average containing 200 points. Let $X \sim PD(k)$ denote that random variable X follows probability distribution PD with parameter k . In particular, $\text{Poisson}(\lambda)$ denotes the Poisson distribution with event rate λ .

Poisson: We first sampled number N of events, where $N \sim \text{Poisson}(\lambda)$. We then sampled N points from a uniform distribution defined on the unit square $[0, 1] \times [0, 1]$. Here $\lambda = 200$.

Normal: Again number N of events was sampled from $\text{Poisson}(\lambda)$, $\lambda = 200$. We then created N coordinate pairs (x, y) , where both x and y are sampled from normal distribution $N(\mu, \sigma^2)$ with mean μ and standard deviation σ . Here $\mu = 0.5$ and $\sigma = 0.2$.

Matern: Poisson process as above was simulated with event rate κ . Obtained points represent parent points, or cluster centers, on the unit square. For each parent, number N of child points was sampled from $\text{Poisson}(\mu)$. A disk of radius r centered on each parent point was defined. Then, for each parent, the corresponding number N of child points were placed on the disk. Child points were distributed by a uniform distributions on the disks. Note that parent points are not part of the actual data set. We set $\kappa=40$, $\mu=5$, and $r = 0.1$.

Thomas: Thomas process is similar to Matern process except that instead of uniform distributions, child points are sampled from bivariate normal distributions defined on the disks. The distributions were centered on the parents and had diagonal covariance $\begin{bmatrix} 0.1^2 & 0 \\ 0 & 0.1^2 \end{bmatrix}$.

Baddeley-Silverman: For this process the unit square was divided into equal size tiles with side lengths $1/14$. Then for each tile, N points were sampled, $N \sim \text{Baddeley-Silverman}$. Baddeley-Silverman distribution is a discrete distribution defined on values $(0, 1, 10)$ with probabilities $(\frac{1}{10}, \frac{8}{9}, \frac{1}{90})$. For each tile, associated number of N points were then uniformly distributed on the tile.

Iterated function system (IFS): We also generated point sets with an iterated function system. For this a discrete distribution is defined on values $(0, 1, 2, 3, 4)$ with corresponding probabilities $(\frac{1}{3}, \frac{1}{6}, \frac{1}{6}, \frac{1}{6}, \frac{1}{6})$. We denote this distribution by IFS. Starting from an initial point (x_0, y_0) on the unit square, $N \sim \text{Poisson}(200)$

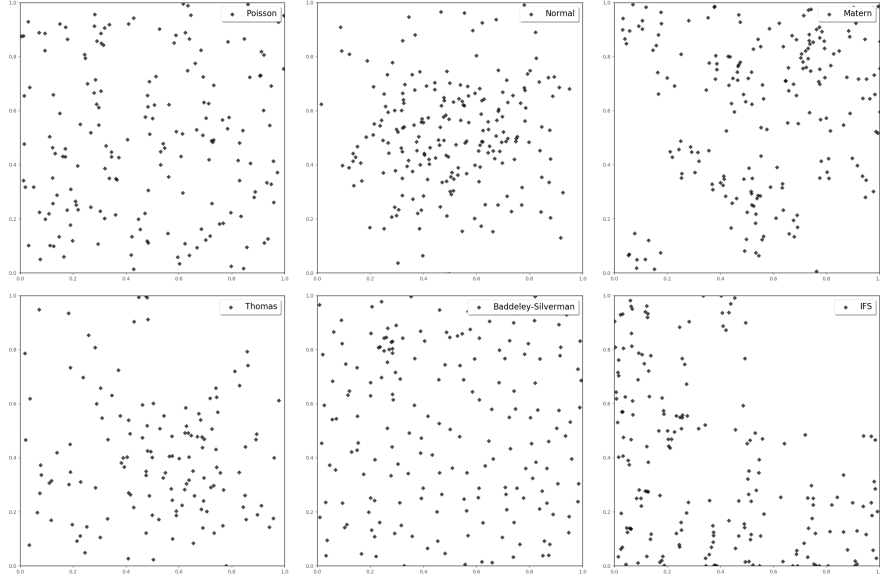


Figure 3: Example realizations of point processes on unit square.

new points were generated by the recursive formula $(x_n, y_n) = f_i(x_{n-1}, y_{n-1})$, where $n \in \{1, \dots, N\}$, $i \sim \text{IFS}$ and the functions f_i are given as

$$f_0(y, x) = \left(\frac{x}{2}, \frac{y}{2}\right), f_1(y, x) = \left(\frac{x}{2} + \frac{1}{2}, \frac{y}{2}\right), f_2(y, x) = \left(\frac{x}{2}, \frac{y}{2} + \frac{1}{2}\right),$$

$$f_3(y, x) = \left(\left|\frac{x}{2} - 1\right|, \frac{y}{2}\right), f_4(y, x) = \left(\frac{x}{2}, \left|\frac{y}{2} - 1\right|\right).$$

Figure 3 shows realizations of the point processes with given parameters. From topological data analysis point of view the point sets hold no distinct large scale topology. It is therefore ideal to study the geometric correlations or features in the filtration captured by homologies in degrees 0 and 1, denoted H_0 and H_1 respectively.

Figure 4 shows H_1 stable ranks from distance and shift contours for one realization of the point processes. Corresponding stem plot and contour lines are shown in Figure 2. Note the different character of stable ranks between contours. Distance contour decreases lifespans of bars relative to it making the stable ranks decrease to zero faster and also diminishing their separation (Figure 4 left). Comparing, for example, Poisson and Baddeley-Silverman point processes in Figure 3, Poisson seems to have larger H_1 features appearing at larger filtration values. The point structure of Baddeley-Silverman seems to indicate that it has smaller H_1 features at smaller filtration values. Shift contour increases lifespans of those smaller Baddeley-Silverman bars around filtration value $s = 0.08$ (right plot in Figure 2) whereas more of the later Poisson bars are shortened by the contour after $s = 0.08$. This can be seen in Baddeley-Silverman dominating Poisson stable rank (Figure 4 right). Note that the horizontal axes in Figure 4 correspond to the t variable of contour $C(s, t)$ while the horizontal axes of stem plots are the filtration values s .

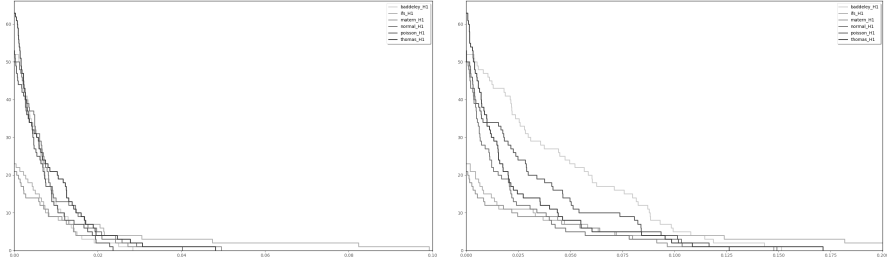


Figure 4: Stable ranks in H_1 of point processes for distance (left) and shift (right) contours of Figure 2. The bars are also shown in the stem plot of Figure 2.

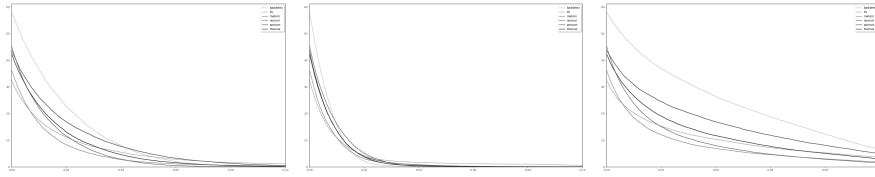


Figure 5: Mean H_1 stable ranks of 200 simulations of point processes with respect to the standard contour (left), distance contour of Figure 2 (middle) and shift contour of Figure 2 (right). All the plots are on the same scale.

Explanation in the previous paragraph exemplifies how the choice of metric allows analyst to emphasize differently homological features in persistence analysis. As referenced in Section 1, various recent applications have shown that bars of different sizes and also their locations in the filtration might be deemed important for a given analysis task. The framework of hierarchical stabilization facilitates this kind of exploration. For instance, consider set of samplings of some dynamical phenomenon. Analysis with contours might help understanding whether observed smaller H_1 features are just sampling noise or indicate actual puncturing of the underlying topology of the dynamics. Quantifying importance of holes is also interesting in relational databases where they indicate missing data values or non-allowed attribute combinations [10].

Figure 5 is a plot of the averages (point-wise means) of H_1 stable ranks with respect to the standard contour and distance and shift contours of Figure 2 for 200 simulations of the point processes. Shift contour increases the separation between the stable ranks as compared to the standard contour, whereas distance contour decreases the separation. It is worth noting that Matern and Thomas processes are well distinguished by the shift contour in the right plot even though in their definition they only differ in the distribution used for point clusters.

To test how well the stable ranks with respect to different contours perform in classifying different point processes we conducted mean classification procedure:

- For each class choose 200 simulations as a training set. Remaining 300 simulations form test set for the class.

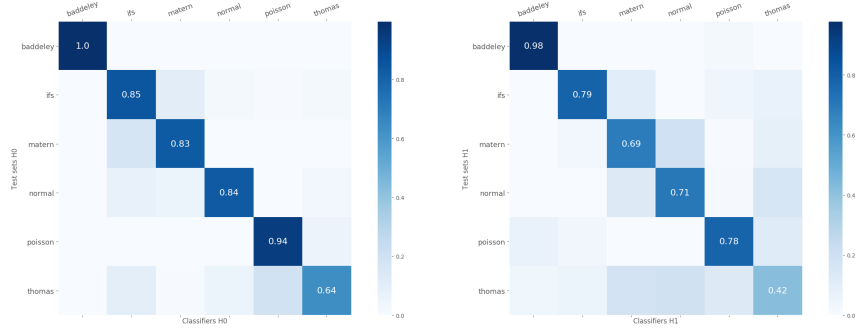


Figure 6: Confusion matrices for the point process classification in H_0 (left) and H_1 (right) with standard contour.

- Compute the point-wise means of the training set stable ranks with respect to the chosen contour. These mean invariants are used as classifiers, denoted by \hat{C}_{H_\bullet} , where H_\bullet refers to the corresponding homology.
- Denote stable ranks in the test set by T_{H_\bullet} . Compute distances $L_1(\hat{C}_{H_\bullet}, T_{H_\bullet})$ between each test element and all classifiers.
- Record found minimum distance by adding 1 to the corresponding pair of the classifier and the test class. Classification is successful if the classifier and the test belong to the same class (in the optimal case the value of the pair (Poisson \hat{C} , Poisson T) would be 300, for example).
- For cross-validation use 20-fold random subsampling. Randomly sample 200 stable ranks for classifiers, remaining 300 stable ranks in each class constitute the test sets. Repeat the classification procedure above 20 times and take the classification accuracy to be the average over the folds.

Cross-validated classification accuracies with standard contour are reported in the confusion matrices of Figure 6. The confusion matrices show relative accuracies after dividing by 300 after each fold and averaging after the full cross-validation run. The mean classification accuracy by taking the average over classes (average of the diagonal) is 85% for H_0 and 73% for H_1 . The classification procedure performs comparably or better as the hypothesis testing against the homogeneous Poisson process in [4]. Note that no other assumptions or parameter selections were involved in our methodology other than the split between training and test samples (200 and 300, respectively.)

Figure 8 shows cross-validated classification accuracies for H_1 stable ranks with shift contour described in Figure 7. We thus increase the lifespans of features appearing in the middle of the filtration. The overall classification accuracy increased to 78%. Particularly classification accuracy of the Thomas process was drastically improved as shown in the confusion matrix of Figure 8. Also noteworthy is the improvement in the accuracy of normal and Poisson processes. Using the shift contour thus captures more relevant distinguishing homological information of the point processes compared to the standard contour.

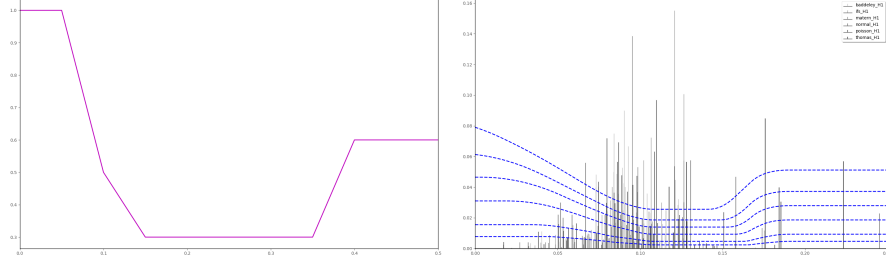


Figure 7: Density function used in producing shift contour for point process classification in H_1 (left). Corresponding contour lines and stem plots from H_1 persistence analysis of one realization of the studied point processes (right).

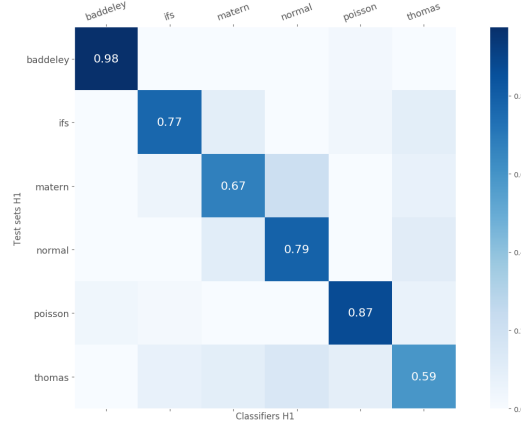


Figure 8: Confusion matrix for the classification of point processes in H_1 with contour coming from density function in Figure 7.

10.3 Activity monitoring

As an application to real data we studied activity monitoring of different physical activities. Used data set was PAMAP2 data obtainable from [14]. It makes sense to use all the persistence information, i.e. to combine homologies of different degrees into single classification scheme. In this section we demonstrate how this is enabled by stable ranks and our pipeline.

The data consisted of seven persons from the PAMAP2 data set performing different activities such as walking, cycling, vacuuming and sitting. Test subjects were fitted with three Inertial Measurements Units (IMUs), one on wrist, ankle and chest, and a heart rate monitor. Measurements were registered every 0.1 seconds. Each IMU measured 3D acceleration, 3D gyroscopic and 3D magnetometer data. One data set thus consisted of 28-dimensional data points indexed by 0.1 second timesteps.

We looked at two activities in this case study: ascending and descending stairs. At the outset one would expect these activities to be very similar and therefore difficult to distinguish. For persistence analysis we randomly sampled without replacement 100 points from each data set, repeated 100 times. For each of the 7 subjects we thus obtained 100 resamplings from their activity

data. We computed H_0 and H_1 persistence for each sampling. The classification procedure was the same as outlined in Section 10.2 except we combined both homologies in the classifier as follows. We took the mean of 40 out of 100 stable ranks both in H_0 and H_1 . We thus obtained 14 classifier pairs $(\hat{C}_{H_0}, \hat{C}_{H_1})$ corresponding to all (subject, activity) classes. Remaining 60 stable ranks formed test data pairs (T_{H_0}, T_{H_1}) in each class. For a pair (T_{H_0}, T_{H_1}) we then considered

$$\min\{L_1(\hat{C}_{H_0}, T_{H_0}) + L_1(\hat{C}_{H_1}, T_{H_1})\} \text{ for each pair } (\hat{C}_{H_0}, \hat{C}_{H_1}).$$

Again the classification is successful if the minimum is obtained with $(\hat{C}_{H_0}, \hat{C}_{H_1})$ and (T_{H_0}, T_{H_1}) belonging to the same (subject, activity) class.

Results for 20-fold random subsampling cross-validation are shown on the left in Figure 9 for the standard contour, with the overall accuracy of 60%. For the classification with a different contour we use the standard contour for H_0 and the shift contour of Figure 10 for H_1 . The results are shown on the right in Figure 9. The shift contour increases lifespans of H_1 features appearing with larger filtration values. Exploring the stem plots (Figure 10) for different data sets shows that larger filtration values have bars sparsely (some data sets having no bars) and their lengths vary significantly between different classes of data. This observation leads to use the contour emphasizing bars in the larger filtration values, by which the classification accuracy increases to 65%. Note particularly increase in the accuracy of subject 4. Also noteworthy is that ascendings mainly get confused with ascendings and the same for descendings. These data thus exhibit clearly different character and using an appropriate contour makes this difference more pronounced.

10.4 Choosing the contour

The examples above illustrate how one does data analysis by choosing a more optimal contour which gives a pseudometric on $\text{Tame}([0, \infty), \text{Vec}_K)$. In the examples this choice was made by visually inspecting stem plots and contour lines. The next step of our pipeline is to automate this process. This is the central reason behind contours and induced metrics: we want to optimize over the space of metrics to find more distinguishing invariants for objects in $\text{Tame}([0, \infty), \text{Vec}_K)$. This leads to optimizing in an appropriate function space since contours arise from density functions (see Section 5). Another way would be to represent densities by functions whose shape is controlled by few parameters, such as a beta distribution with shape parameters α and β . The optimization then reduces to these parameters.

A Proofs of Propositions from Section 2

Proof of Proposition 2.1. (1): If $d(X, Y) = \infty$, there is nothing to prove. Assume $\epsilon := d(X, Y) < \infty$. For t in $[0, \infty)$, there are inclusions $B(Y, t) \subset B(X, t + \epsilon)$ and $B(X, t) \subset B(Y, t + \epsilon)$ which imply $\hat{R}_d(Y)(t) \geq \hat{R}_d(X)(t + \epsilon)$ and $\hat{R}_d(X)(t) \geq \hat{R}_d(Y)(t + \epsilon)$. As this happens for all t , we can conclude $\epsilon \geq d_{\infty}(\hat{R}_d(X), \hat{R}_d(Y))$.

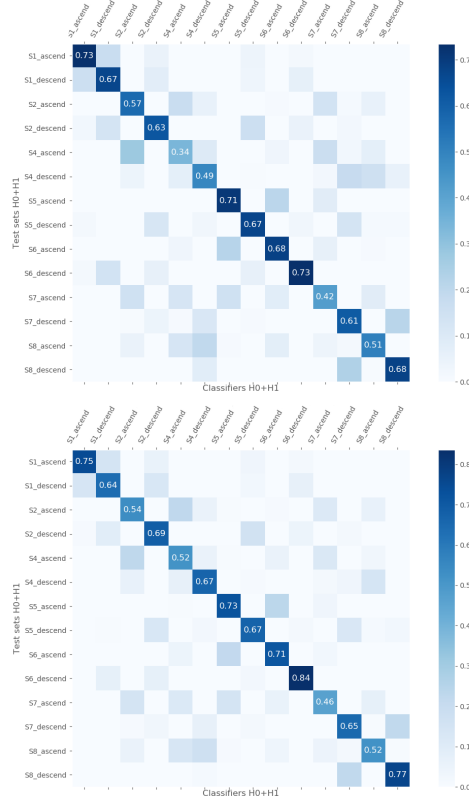


Figure 9: Confusion matrix for the classification of ascending and descending stairs activities with standard contour (left). Confusion matrix for the classification of ascending and descending stairs activities with contour coming from density function of Figure 10 (right).

(2): Using (1), it is enough to prove that, for non-increasing functions f and g :

$$\max\{f(0), g(0)\} d_{\infty}(f, g)^{\frac{1}{p}} \geq L_p(f, g).$$

The inequality is clear if $d_{\infty}(f, g) = \infty$. Assume there is ϵ such that $f(t) \geq g(t + \epsilon)$ and $g(t) \geq f(t + \epsilon)$ for any t . This together with the fact that f and g are non-increasing imply $h \geq f \geq h_{\epsilon}$ and $h \geq g \geq h_{\epsilon}$ where $h = \max\{f, g\}$ and h_{ϵ} is the function $t \mapsto h(t + \epsilon)$. The desired inequality is then a consequence of h being non-increasing and the fact $(b - a)^p \leq b^p - a^p$ for $a \leq b$ in $[0, \infty)$ and $p \geq 1$ which give:

$$\begin{aligned} L_p(h, h_{\epsilon})^p &= \int_0^{\infty} (h(t) - h_{\epsilon}(t))^p dt \leq \int_0^{\infty} h(t)^p - h_{\epsilon}(t)^p dt = \\ &= \int_0^{\epsilon} h(t)^p dt \leq h(0)^p \epsilon = \max\{f(0), g(0)\}^p \epsilon. \end{aligned}$$

□

Proof of Proposition 2.2. Let $\{d_{\alpha}\}_{\alpha \in [0, \infty]}$ be a non-decreasing sequence of pseudometrics on T . Choose ϵ in $(0, \infty)$. For α in $(0, \infty)$, set $\lfloor \alpha / \epsilon \rfloor$ to be the biggest

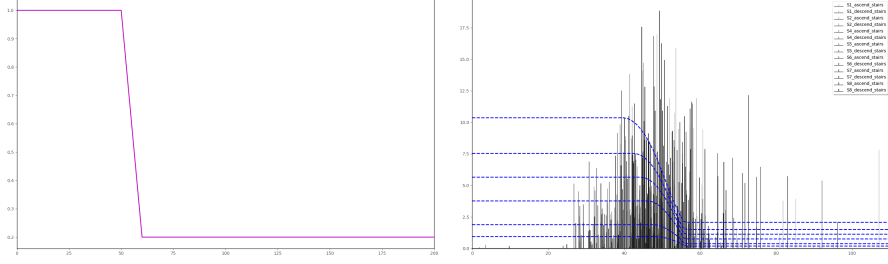


Figure 10: Density function used for H_1 stable ranks in the activities classification (left) and contour lines and persistence stem plots for single data sets (right).

natural number not bigger than α/ϵ . Define $d_\alpha^\epsilon := d_{\lfloor \alpha/\epsilon \rfloor \epsilon}$ and $d_\infty^\epsilon := d_\infty$. In this way, any ϵ leads to a new non-decreasing sequence $\{d_\alpha^\epsilon\}_{\alpha \in [0, \infty]}$ of pseudometrics on T . This new sequence is also non-decreasing. Let $\bar{R}_\epsilon(X) : [0, \infty)^2 \rightarrow [0, \infty)$ be the function corresponding to this new sequence as defined in 2.2.(2). Since $\{d_\alpha^\epsilon\}_{\alpha \in [0, \infty]}$ is constant on intervals of the form $[n\epsilon, (n+1)\epsilon)$ where n is a natural number, the function $\bar{R}_\epsilon(X) : [0, \infty)^2 \rightarrow [0, \infty)$ is Lebesgue measurable as it is constant on left closed rectangles that cover $[0, \infty)^2$. Note that $\bar{R}(X)$ is the limit of $\bar{R}_\epsilon(X)$ as ϵ goes to 0. As a limit of measurable functions, $\bar{R}(X)$ is then also measurable. \square

Proof of Proposition 2.3. Since to prove this proposition one can use exactly the same arguments as in the proof of Proposition 2.1, we illustrate how to show statement (1) only. If $d_\infty(X, Y) = \infty$, then the statement is clear. Assume $\epsilon := d_\infty(X, Y) < \infty$. Since $\{d_\alpha\}_{\alpha \in [0, \infty]}$ is non-decreasing, for any (α, t) in $[0, \infty) \times [0, \infty)$, we have an inclusion $B_{d_\alpha}(Y, t) \subset B_{d_\alpha}(X, t + \epsilon)$ which yields $\bar{R}(Y)(\alpha, t) \geq \bar{R}(X)(\alpha, t + \epsilon)$. By symmetry also $\bar{R}(X)(\alpha, t) \geq \bar{R}(Y)(\alpha, t + \epsilon)$, and hence $\epsilon \geq d_\infty(\bar{R}(X), \bar{R}(Y))$. \square

References

- [1] U. Bauer. Ripser software. github.com/Ripser/ripser.
- [2] P. Bendich, S. Chin, J. Clarke, J. Desena, J. Harer, E. Munch, A. Newman, D. Porter, D. Rouse, N. Strawn, and A. Watkins. Topological and statistical behavior classifiers for tracking applications. *IEEE Transactions on Aerospace and Electronic Systems*, 52:2644–2661, 2016.
- [3] P. Bendich, J. Marron, E. Miller, A. Pieloch, and S. Skwerer. Persistent homology analysis of brain artery trees. *The Annals of Applied Statistics*, 10:198–218, 2016.
- [4] C. Biscio and J. Møller. The accumulated persistence function, a new useful functional summary statistic for topological data analysis, with a view to brain artery trees and spatial point process applications. *arXiv:1611.00630*, 2016.

- [5] Peter Bubenik, Vin de Silva, and Jonathan Scott. Metrics for generalized persistence modules. *Foundations of Computational Mathematics*, 15(6):1501–1531, 2015.
- [6] Oliver Gäfvert. Algorithms for multidimensional persistence. *Master’s Thesis, KTH*, 2016.
- [7] Oliver Gäfvert and Wojciech Chachólski. Stable invariants for multidimensional persistence. *arXiv:1703.03632*, 2017.
- [8] Y. Hiraoka, T. Nakamura, A. Hirata, E. Escolar, K. Matsue, and Y. Nishiura. Hierarchical structures of amorphous solids characterized by persistent homology. *Proceedings of the National Academy of Sciences*, 113:7035–7040, 2016.
- [9] Y. Hiraoka, T. Shirai, and K. D. Trinh. Limit theorems for persistence diagrams. *The Annals of Applied Probability*, 28:2740–2780, 2018.
- [10] R. Andonie J. Lemley, F. Jagodzinski. Big holes in big data: A monte carlo algorithm for detecting large hyper-rectangles in high dimensional data. *IEEE 40th Annual Computer Software and Applications Conference*, pages 563–571, 2016.
- [11] D. Meyer K. Meehan. An isometry theorem for generalized persistence modules. *arXiv:1710.02858*, 2017.
- [12] L. Kanari, P. Dlotko, M. Scolamiero, R. Levi, J. Shillcock, K. Hess, and H. Markram. A topological representation of branching neuronal morphologies. *Neuroinformatics*, 16:3–13, 2018.
- [13] Y. Lee, S. Barthel, P. Dlotko, S.M. Moosavi, K. Hess, and B. Smit. Quantifying similarity of pore-geometry in nanoporous materials. *Nature Communications*, 8(15396), 2017.
- [14] PAMAP. Physical activity monitoring for aging people. www.pamap.org.
- [15] V. Puuska. Erosion distance for generalized persistence modules. *arXiv:1710.01577*, 2017.
- [16] A. Robinson and K. Turner. Hypothesis testing for topological data analysis. *Journal of Applied and Computational Topology*, 1:241–261, 2017.
- [17] Martina Scolamiero, Wojciech Chachólski, Anders Lundman, Ryan Ramanujam, and Sebastian Öberg. Multidimensional persistence and noise. *Foundations of Computational Mathematics*, 17(6):1367–1406, 2017.
- [18] B. Stolz, H. Harrington, and M. Porter. Persistent homology of time-dependent functional networks constructed from coupled time series. *Chaos*, 27:047410–1 – 047410–17, 2017.
- [19] K. Xia and G.-W. Wei. Persistent homology analysis of protein structure, flexibility, and folding. *International Journal for Numerical Methods in Biomedical Engineering*, 30:814–844, 2014.
- [20] K. Xia and G.-W. Wei. Persistent topology for cryo-em data analysis. *International Journal for Numerical Methods in Biomedical Engineering*, 31, 2015.